Electronic Supplementary Material (ESI) for New Journal of Chemistry.

Supporting Information for:

Isolation of Gravimetrically Quantifiable Alkali Metal Arenides using 18-crown-6

Maximiliano Castillo, Skye Fortier and Alejandro J. Metta-Magana*

General Considerations. All air and moisture sensitive operations were performed in an M. Braun dry box under an atmosphere of purified nitrogen or using high vacuum standard Schlenk techniques. DME, Hexanes and THF were dried using a Pure Process Technology Solvent Purification System and subsequently stored under a dinitrogen atmosphere over activated 4 Å molecular sieves. 18-crown-6 was purchased from Oakwood Products, Inc. and made anhydrous using the Gokel method.[1] IR data were collected using a Thermo Scientific Nicolet iS5 spectrometer. UV-vis/NIR spectra were recorded on a Cary 5000 spectrophotometer.

Cyclic Voltammetry. Cyclic voltammetric measurements were performed using a CH Instruments 600e potentiostat with a PC unit controlled with CHI software (version 13.12). Experiments were performed in a glovebox under an inert N_2 atmosphere using platinum disks (2 mm diameter), embedded in Kel-F thermoplastic, as the counter and working electrodes while the reference electrode consisted of a platinum wire. Solutions utilized in the electrochemical studies were approximately 1 mM in arene complex with $[NBu_4][PF_6]$ (0.1M, THF) as supporting electrolyte. All potentials are reported versus the $[Cp_2Fe]^{0/+}$ couple, referenced as internal standard.

X-ray Crystallography. Data for **1-12** was collected on a Bruker 3-axis platform diffractometer equipped with a APEX I CCD detector using a graphite monochromater with a Mo Kα X-ray source (α = 0.71073 Å). The crystal was mounted on a Mitigen Kapton loop, coated in NVH oil, and maintained at 100(2) K under a flow of nitrogen gas during data collection. A hemisphere of data was collected using ω and φ scans with 0.3º frame widths. Data collection and cell parameter determination were conducted using the SMART program.[2] Integration of the data and final cell parameter refinements were performed using SAINT[3] software with data absorption correction implemented through SADABS.[4] Structures were solved using direct,

charge flipping, or structure expansion methods and difference Fourier techniques. All hydrogen atom positions in **1-12** were idealized and rode on the atom. Structure solution, refinement, graphics, and creation of publication materials were performed using SHELXTL[5] or the Olex2 crystallographic package.[6]

Some of the coordinated THF molecules in **4-6** and **12** exhibit slight positional disorder which was addressed by modeling the disordered atoms over two orientations in a 50:50 ratio. A summary of relevant crystallographic data is presented in Table S1. Weak diffraction data precluded satisfactory structure refinement of **7**; however, a diagram illustrating its connectivity, based up the diffraction data, is shown in Figure S7.

General synthesis of [M(18-crown-6)(solvent)$_x$]Arene$^-$. To a stirring solution of the aromatic hydrocarbon in THF was added freshly cut alkali metal in pieces. The reaction was left to stir for 4 h during which time the reaction mixture turned a dark, deep color. At this stage, any unreacted metal was removed and 18-crown-6 was added to the solution as a solid. After addition of the crown ether, the reaction mixture was stirred for 15 minutes. Storage of this solution at -25 ^{o}C for 12 hours afforded a crop of crystals. The mixture was poured over a medium porosity glass frit and the collected crystals were washed with cold (-25 ^{o}C) THF (1 x 5 mL) and cold (-25 ^{o}C) hexanes (1 x 5 mL). The solid was dried under vacuum to give dark crystalline material.

[Li(18-c-6)][C$_{10}$H$_8$] (1) The synthesis of **1** was performed using 0.113 g (0.881 mmol) of $C_{10}H_8$ and 0.006 g (0.864mmol) of lithium metal in 5 mL of THF to which 0.228 g (0.864 mmol) of 18-crown-6 was added. Yield: 0.128 g, 37%. Dark green crystals of **1** for X-ray crystallographic analysis were grown from a concentrated dark green THF solution stored at -25 ^{o}C. 1.53 μ_B (Gouy measurement). UV-vis/NIR (THF, 0.106 mM, 25 °C, L•mol^{-1}•cm^{-1}): 294 (ε = 9173), 318 (ε = 4230), 327 (ε = 6584), 376 (ε = 2812), 419 (sh, ε = 1904), 435 (ε = 1764), 468 (ε = 1089) 799 (ε = 1284). IR (KBr pellet): 3673(w), 3435(w), 3046(m), 3010(m), 2978(m), 2910(s), 2859(s), 2875(s), 2823(m), 2798(m), 2744(m), 2705(m), 2539(w), 2479(w), 2404(w), 2370(w), 2343(w), 2238(w), 2166(w), 2132(w), 1970(w), 1940(w), 1772(w), 1671(w), 1612(m), 1593(m), 1500(m), 1477(s), 1457(s), 1390(m), 1350(s), 1292(m), 1283(m), 1244(s), 1187(s), 1107(s), 1006(w), 993(m), 964(w), 927(m), 894(w), 836(m), 809(s), 783(m), 734(w), 711(m), 617(w), 593(m), 565(w), 531(w), 512(w), 482(m), 471(m), 441(w), 419(w).

[Na(18-c-6)DME][$C_{10}H_8$] (2) While the initial synthesis of **2** was performed using THF followed by recrystallization from DME, it was found that the reaction can be performed in DME from the outset. Accordingly, **2** was synthesized using 0.142 g (1.107 mmol) of $C_{10}H_8$ and 0.023 g (1.000 mmol) of sodium metal in 5 mL of DME to which 0.262 g (0.991 mmol) of 18-crown-6 was added. Yield: 0.400 g, 79%. Dark green crystals of **2** for X-ray crystallographic analysis were grown from a concentrated dark green DME solution stored at -25 ^{o}C. 1.67 μ_B (Gouy measurement). UV-vis/NIR (THF, 0.139 mM, 25 °C, L•mol^{-1}•cm^{-1}): 294 (ε = 10709), 322 (sh, ε = 5364), 327 (ε =9057), 373 (ε = 3140), 409 (sh, ε = 1900), 442 (ε = 1560), 455 (sh, ε = 1363), 469 (ε = 1125), 695 (sh, ε = 1133), 798 (ε = 1650), 875 (ε = 1545) . IR (KBr pellet): 3046(m), 3015(m), 2904(s), 2890(s), 2821(m), 2794(w), 2743(w), 2706(w), 1972(w), 1593(w), 1495(w), 1490(m), 1473(m), 1454(m), 1389(w), 1351(s), 1284(m), 1248(m), 1185(s), 1100(s), 1009(w), 996(s), 963(s), 837(m), 808(m), 787(m), 714(m), 617(w), 594(w), 531(w), 482(w).

[K(18-c-6)][μ:η^2-$C_{10}H_8$]}$_\infty$ (3) The synthesis of **3** was performed using 0.103.8 g (0.810 mmol) of $C_{10}H_8$ and 31.7 g (0.810 mmol) of potassium metal in 8 mL of THF to which 0.215 g (0.813 mmol) of 18-crown-6 was added. Yield: 0.280 g, 80%. Dark green crystals of **3** for X-ray crystallographic analysis were grown from a concentrated dark green THF solution stored at -25 ^{o}C. 2.11 μ_B (Gouy measurement). UV-vis/NIR (THF, 0.114 mM, 25 °C, L•mol^{-1}•cm^{-1}): 294 (ε = 6190), 321 (sh, ε = 2753), 326 (ε = 4643), 374 (ε =1574), 408 (sh, ε = 948), 445 (ε = 787), 452 (sh, ε = 715), 469 (ε = 579), 688 (sh, ε = 511), 771 (ε = 811), 856 (ε = 793). IR (KBr pellet): 3046(m), 3015(s), 2935(m), 2883(s), 2853(s), 2821(s), 2792(m), 2742(m), 2712(m), 2687(w), 2537(w), 2485(w), 2406(w), 2386(w), 2349(w), 2286(w), 2245(w), 2166(w), 2133(w), 1972(w), 1944(w), 1834(w), 1764(w), 1693(w), 1668(w), 1593(m), 1492(s), 1464(s), 1454(s), 1431(s),

1364(s), 1350(s), 1282(s), 1252(s), 1235(m), 1187(s), 1101(s), 1057(m), 997(s), 959(s), 838(s), 801(m), 786(m), 712(s), 594(m), 527(w), 464(m).

[Li(κ^3-18-c-6)(THF)$_2$][$C_{12}H_{10}$] (4) The synthesis of **4** was performed using 0.300 g (1.945 mmol) of $C_{12}H_{10}$ and 0.014 g (1.945 mmol) of lithium metal in 6 mL of THF to which 0.524 g (1.982 mmol) of 18-crown-6 was added. Yield: 0.352 g, 42%. Dark indigo crystals of **4** for X-ray crystallographic analysis were grown from a concentrated dark turquoise THF solution stored at -25 ^{o}C. 2.08 μ_B (Gouy measurement). UV-vis/NIR (THF, 0.284 mM, 25 °C, L•mol^{-1}•cm^{-1}): 411 (ε = 12987), 451 (sh, ε = 3433), 609 (sh, ε = 5163), 643 (ε = 5765), 748 (sh, ε = 1971), 829 (ε = 1135). IR (KBr pellet): 3039(s), 2912(s), 2871(s), 2721(w), 2621(w), 2584(w), 2520(w), 2407(w), 1849(w), 1729(w), 1654(w), 1567(s), 1367, 1461(m), 1460(s), 1451(m), 1372(m), 1326(m), 1323(s), 1295(w), 1292(w), 1288(m), 1277(m), 1243(m), 1161(s), 1110(s), 1069(s), 1051(s), 1029(m), 988(s), 987(s), 963(m), 935(m), 892(w), 891(w), 775(m), 729(w), 728(w), 687(w), 668(s), 568(w), 523(w), 421(w).

[Na(18-c-6)(THF)$_2$][$C_{12}H_{10}$] (5) The synthesis of **5** was performed using 0.222 g (1.439 mmol) of $C_{12}H_{10}$ and 0.030 g (1.304 mmol) of sodium metal in 8 mL of THF to which 0.344 g (1.304 mmol) of 18-crown-6 was added. Yield: 0.413 g, 53%. Dark indigo crystals of **5** for X-ray crystallographic analysis were grown from a concentrated dark turquoise THF solution. 2.24 μ_B (Gouy measurement). UV-vis/NIR (THF, 0.284 mM, 25 °C, L•mol^{-1}•cm^{-1}): 410 (ε = 11579), 451 (ε = 5911), 610 (ε = 6420), 653 (ε = 3260), 747 (ε = 1611), 837 (ε = 589). IR (KBr pellet): 3031(w), 2989(w), 2898(s), 2823(w), 2749, 1930(w), 1561(s), 1480(m), 1430(m), 1351(s), 1321(m), 1284(m), 1251(s), 1158(s), 1104(s), 1004(w), 987(m), 963(s), 936(s), 838(s), 778(w), 741(m), 729(s), 699(m), 688(w), 663(w), 610(w), 530(w).

[K(18-c-6)(THF)$_2$][$C_{12}H_{10}$] (6) The synthesis of **6** was performed using 0.268 g (1.744 mmol) of $C_{12}H_{10}$ and 0.068 g (1.744 mmol) of potassium metal in 5 mL of THF to which 0.460 g (1.740 mmol) of 18-crown-6 was added. Yield: 0.400 g, 38%. Dark indigo crystals of **6** for X-ray crystallographic analysis were grown from a concentrated dark turquoise THF solution stored at -25 ^{o}C. 2.20 μ_B (Gouy measurement). UV-vis/NIR (THF, 0.284 mM, 25 °C, L•mol^{-1}•cm^{-1}): 403 (ε = 13327), 435 (ε = 6961), 610 (ε = 5073), 649 (ε = 5641), 747 (ε = 1086), 831 (ε = 907). IR (KBr pellet): 3045(m), 2992(m), 2884(s), 2820(m), 2793(m), 2743(w), 2710(w), 2687(w), 2620(w), 2587(w), 2522(w), 2404(w), 2304(w), 2244(w), 2102(w), 2046(m), 1975(w), 1914(w), 1846(w), 1728(w), 1654(w), 1565(s), 1500(w), 1493(m), 1467(s), 1452(m), 1431(w), 1379(m), 1350(s), 1322(s), 1283(m), 1248(m), 1201(w), 1152(s), 1100(s), 1060(m), 1004(m), 987(s), 962(s), 936(s), 905(w), 838(m), 772(w), 742(w), 707(w), 688(w), 671(s), 549(w), 536(w), 530(w).

[Li(18-c-6)][$C_{14}H_{10}$] (7) The synthesis of **7** was performed using 0.102 g (0.572 mmol) of $C_{14}H_{10}$ and 0.003 g (0.432mmol) of lithium metal in 3 mL of THF to which 0.139 g (0.525 mmol) of 18-crown-6 was added. Yield: 0.070 g, 30%. Dark blue crystals of **7** for X-ray crystallographic analysis were grown from a concentrated dark blue DME solution layered with hexanes and stored at -25 ^{o}C. 1.67 μ_B (Gouy measurement). UV-vis/NIR (THF, 0.105 mM, 25 °C, L•mol^{-1}•cm^{-1}): 328 (ε = 21450), 340 (ε = 10142), 348 (ε = 10019), 358 (ε = 11087), 369 (ε = 18888), 378 (ε = 5705), 407 (ε = 2464), 478 (ε = 783), 513 (ε = 1046), 550 (ε = 1543), 585 (ε = 1892), 598 (ε = 2245), 641 (ε = 2542), 659 (ε = 3478), 696 (ε = 4726), 735 (ε = 5918), 759 (ε = 5752), 813 (ε = 1452), 843, (ε = 966), 921 (ε = 622), 956 (ε = 392). IR (KBr pellet): 3057(w), 3033(m), 3002(m), 2965(m), 2909(s), 2873(s), 2731(w), 2709(w), 2677(m), 2580(w), 2555(w), 2529(w), 2487(w), 2455(w), 2357(w), 2268(w), 2156(w), 2116(w), 2045(w), 1840(m), 1769(w),

1753 (m), 1697(w), 1648(m), 1560(m), 1512(s), 1463(s), 1450(s), 1378(s), 1364(m), 1320(s), 1293(s), 1280(s), 1264(s), 1243(m), 1189(w), 1170(s), 1153(s), 1113(s), 1068(s), 1049(s), 1021(s), 963(w), 932(s), 897(w), 883(m), 836(w), 823(w), 799(s), 772(s), 726(w), 701(m), 692(s), 620(w), 590(w), 588(w), 569(w), 518(m), 460(s), 421(w).

[Na(18-c-6)(DME)][$C_{14}H_{10}$] (8) The synthesis of **8** was performed using 0.246 g (1.380 mmol) of $C_{14}H_{10}$ and 0.034 g (1.478mmol) of sodium metal in 8 mL of DME to which 0.400 g (1.513 mmol) of 18-crown-6 was added. Yield: 0.673 g, 87%. Dark blue crystals of **8** for X-ray crystallographic analyses were grown from a concentrated dark blue DME solution stored at -25 ^{o}C. 1.90 μ_B (Gouy measurement). UV-vis/NIR (THF, 0.115 mM, 25 °C, L•mol^{-1}•cm^{-1}): 328 (ε = 26757), 349 (ε = 12184), 363 (ε = 11631), 368 (ε = 23879), 378 (sh, ε = 4411), 406 (sh, ε = 2749), 475 (ε = 875), 512 (ε = 1274), 539 (sh, ε = 1835), 553 (ε = 2054), 588 (ε = 2589), 599 (ε = 2927), 642 (sh ε = 3412), 663 (ε = 4519), 699 (ε = 6340), 734 (ε = 8185), 761 (ε = 7764), 819 (ε = 1871), 837 (ε = 1360), 934 (ε = 739). IR (KBr pellet): 3039(w), 3033(w), 3005(w), 2893(s), 2867(s), 2740(w), 2675(w), 1831(w), 1784(w), 1748(w), 1636(w), 1620(w), 1561(w), 1534(w), 1512(m), 1452(m), 1449(m), 1379(s), 1375(m), 1320(s), 1288(m), 1249(m), 1169(m), 1101(s), 1019(m), 997(w), 963(s), 883(s), 836(m), 798(m), 738(m), 744(m), 726(s), 699(m), 602(w), 531(w), 474(m), 461(w).

[K(18-c-6)(THF)$_2$][$C_{14}H_{10}$] (9) The synthesis of **9** was performed using 0.115 g (0.645 mmol) of $C_{14}H_{10}$ and 0.025 g (0.639 mmol) of potassium metal in 8 mL of DME to which 0.148 g (0.559 mmol) of 18-crown-6 was added. Yield: 0.225 g, 64%. Dark blue crystals of **9** for X-ray crystallographic analyses were grown from a concentrated dark blue THF solution stored at -25 ^{o}C. 1.97 μ_B (Gouy measurement). UV-vis/NIR (THF, 0.116 mM, 25 °C, L•mol^{-1}•cm^{-1}): 328 (ε = 30268), 340 (sh, ε = 14422), 348 (ε = 14570), 358 (ε = 13896), 367 (ε = 27078), 378 (sh, ε =

5275), 407 (ε = 3746), 478 (sh, ε = 1003), 513 (sh, ε = 1496), 550 (ε = 2489), 585 (sh, ε = 2651), 598 (ε = 3600), 640 (ε = 3953), 661 (ε = 5661), 698 (ε = 7691), 733 (ε = 9709), 759 (ε = 8589), 813 (ε = 2098), 843 (sh, ε = 1442), 925 (ε = 919), 956 (sh, ε = 521). IR (KBr pellet): 3501(w), 3013(m), 2916(m), 2883(s), 2879(s), 2822(m), 2810(m), 2741(m), 2689(m), 2678(m), 1837(w), 1790(w), 1744(m), 1562(m), 1523, 1514(s), 1469(s), 1450(s), 1430(m), 1383(s), 1375(s), 1320(s), 1282(s), 1245(s), 1241(s), 1179(w), 1170(s), 1127(s), 1099(s), 1059(s), 1020(s), 962(s), 849(s), 803(s), 800(s), 774(s), 738(s), 709(s), 702(s), 602(w), 529(w), 470(s).

[Li(κ^3-18-c-6)(DME)][$C_{20}H_{12}$]•0.5$C_{20}H_{12}$ (10) The synthesis of **10** was performed using 0.224 g (0.887 mmol) of $C_{20}H_{12}$ and 0.006 g (0.864 mmol) of lithium metal in 8 mL of THF to which 0.250 g (0.945 mmol) of 18-crown-6 was added. Yield: 0.361 g, 55%. Dark purple crystals of **10** for X-ray crystallographic analyses were grown from a concentrated dark blue-purple DME solution stored at -25 ^{o}C. 2.20 μ_B (Gouy measurement). UV-vis/NIR (THF, 0.036 mM, 25 °C, L•mol^{-1}•cm^{-1}): 322 (ε = 13169), 376 (sh, ε = 3502), 392 (ε = 6108), 411 (ε = 12220), 437 (ε = -16010), 536 (sh, ε = 7123), 579 (ε = 40270), 688 (ε = 3809), 740 (ε = 3308), 761 (ε = 3342), 782 (ε = 3105), 813 (ε = 2782), 847 (ε = 2653), 882 (sh, ε = 2215), 903 (ε = 2466), 1007 (ε = 1088). IR (KBr pellet): 3064(w), 3049(m), 2903(s), 2871(s), 1591(w), 1563(w), 1535(s), 1480(w), 1468(m), 1455(m), 1405(w), 1380(m), 1364(m), 1352(m), 1310(s), 1280(s), 1250(m), 1215(w), 1185(w), 1108(s), 1071(s), 1051(m), 1019(m), 964(m), 931(w), 898(w), 837(w), 811(s), 788(m), 766(s), 748(s), 585(w), 568(w), 541(w), 529(w), 465(w), 458(w).

[Na(18-c-6)(DME)][$C_{20}H_{12}$] (11) The synthesis of **11** was performed using 0.114 g (0.564 mmol) of $C_{20}H_{12}$ and 0.017 g (0.739 mmol) of sodium metal in 8 mL of DME to which 0.198 g (0.564 mmol) of 18-crown-6 was added. Yield: 0.300 g, 84%. Dark purple crystals of **11** for X-ray crystallographic analyses were grown from a concentrated dark blue-purple DME solution

stored at -25 ^{o}C. 2.29 μ_B (Gouy measurement). UV-vis/NIR (THF, 0.052 mM, 25 °C, L•mol^{-1}•cm^{-1}): 323 (ε = 11424), 375 (sh, ε = 3734), 393 (ε = 5298), 414 (ε = 8664), 438 (ε = 13276), 465 (ε = 8595), 535 (sh, ε = 7418), 580 (ε = 33319), 692 (ε = 5764), 737 (ε = 4688), 761 (sh, ε = 4503), 782 (ε = 2669), 813 (ε = 2512), 849 (ε = 2193), 882 (sh, ε = 2119), 906 (ε = 2410), 1010 (ε = 1103). IR (KBr pellet): 3085(w), 3048(m), 3032(m), 2894(s), 2872(s), 1969(w), 1923(w), 1863(w), 1564(m), 1548(m), 1534(s), 1494(w), 1469(m), 1405(w), 1392(w), 1380(w), 1350(s), 1330(m), 1312(s), 1280(s), 1250(s), 1215(w), 1203(w), 1184(w), 1125(s), 1103(s), 1019(s), 962(s), 949(s), 862(w), 840(m), 811, 788(m), 767(s), 749(s), 541(w), 529(w), 487(w), 457(w).

[K(18-c-6)(THF)$_2$][C$_{20}$H$_{12}$] (12) The synthesis of **12** was performed using 0.488 g (2.415 mmol) of $C_{20}H_{12}$ and 0.071 g (1.815 mmol) of potassium metal in 8 mL of DME to which 0.486 g (1.838 mmol) of 18-crown-6 was added. Yield: 0.480 g, 38%. Dark purple crystals of **12** for X-ray crystallographic analyses were grown from a concentrated dark blue-purple THF solution stored at -25 ^{o}C. 2.10 μ_B (Gouy measurement). UV-vis/NIR (THF, 0.056 mM, 25 °C, L•mol^{-1}•cm^{-1}): 323 (ε = 18863), 371 (sh, ε = 3845), 393 (ε = 5272), 413 (ε = 8311), 438 (ε = 10908), 468 (sh, ε = 1733), 532 (sh, ε = 10780), 580 (ε = 58459), 689 (ε = 6518), 741 (ε = 6111), 757 (ε = 6257), 778 (ε = 5957), 812 (ε = 4993), 847 (ε = 4966), 885 (sh, ε = 4385), 903 (ε = 4474), 1008 (ε = 2291). IR (KBr pellet): 3501(w), 3085(w), 3031(m), 2881(s), 2825(s), 2745(s), 1971(w), 1871(w), 1688(w), 1638(w), 1620(w), 1564(s), 1548(s), 1536(s), 1466(s), 1450(m), 1431(w), 1406(w), 1392(w), 1365(w), 1350(s), 1331(s), 1311(s), 1283(s), 1262(s), 1253(s), 1205(w), 1133(s), 1105(s), 1020(s), 992(w), 961(s), 839(s), 811(w), 802(m), 788(s), 752(s), 568(w), 532(w), 526(w), 489(w), 455(m)..

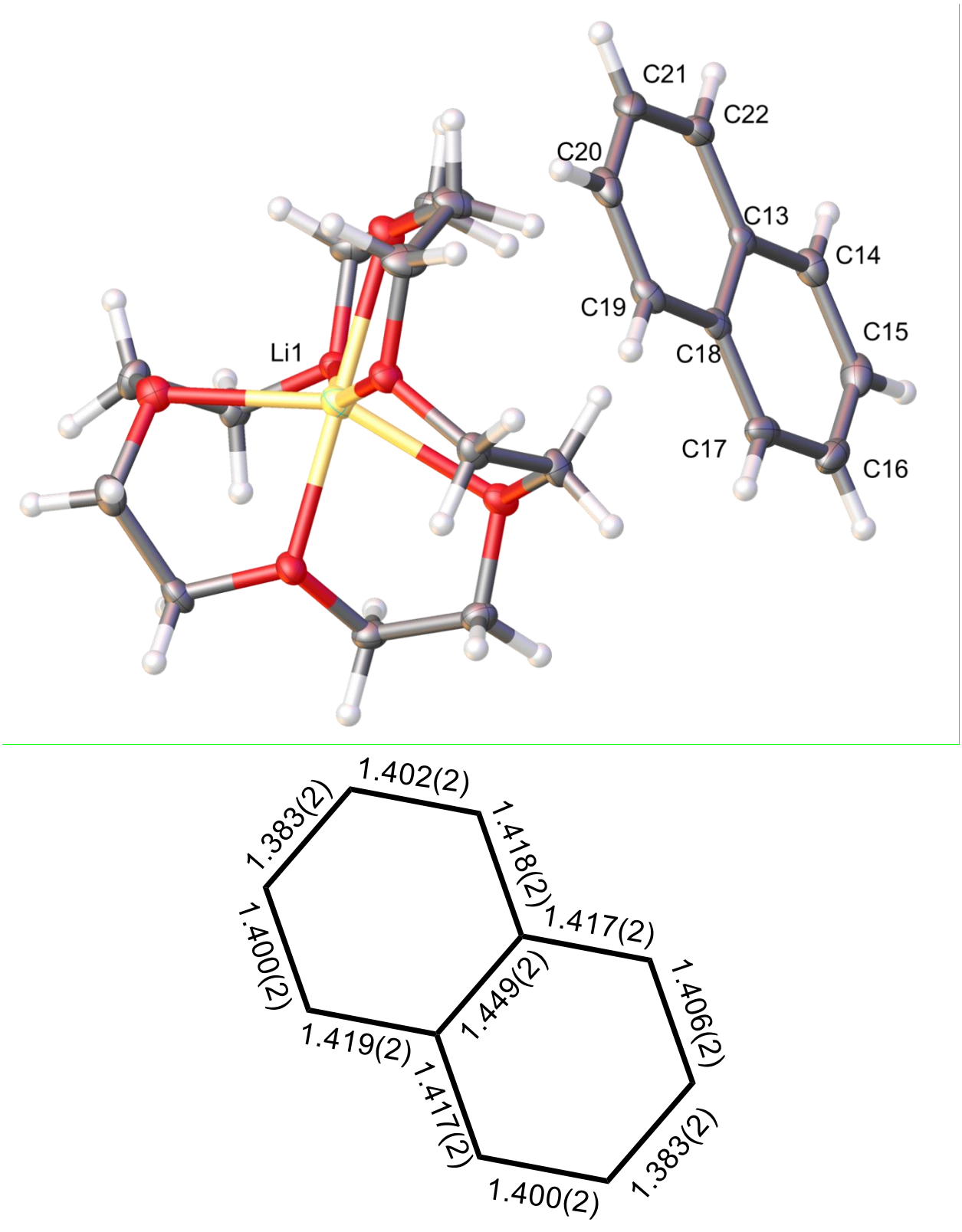

Figure S1. Solid-state molecular structure of **1** with 50% probability ellipsoids and respective bond length (Å) diagram.

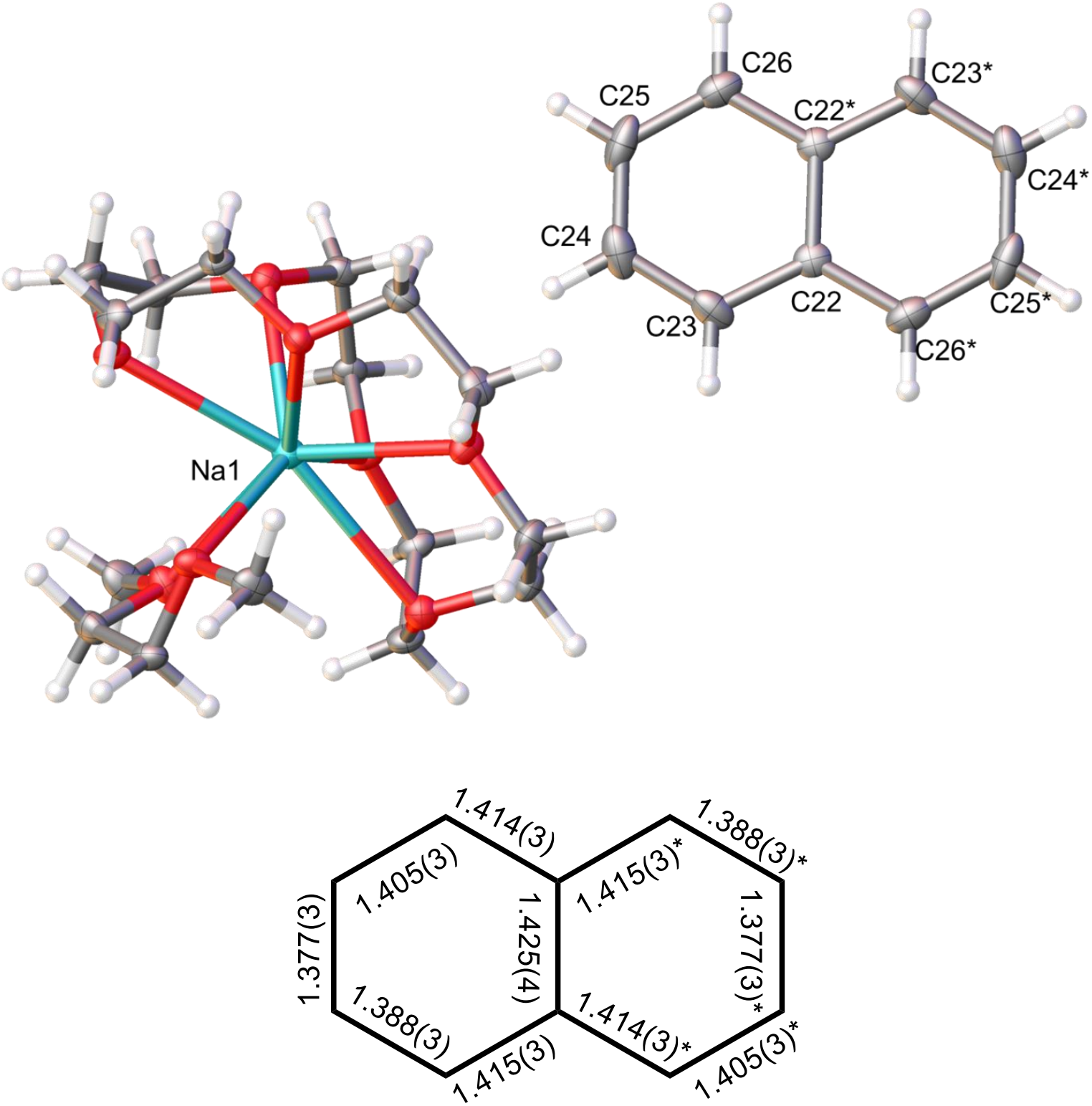

Figure S2. Solid-state molecular structure of **2** with 50% probability ellipsoids and respective bond length (Å) diagram. Asterisks denote symmetry generated atoms and bond lengths.

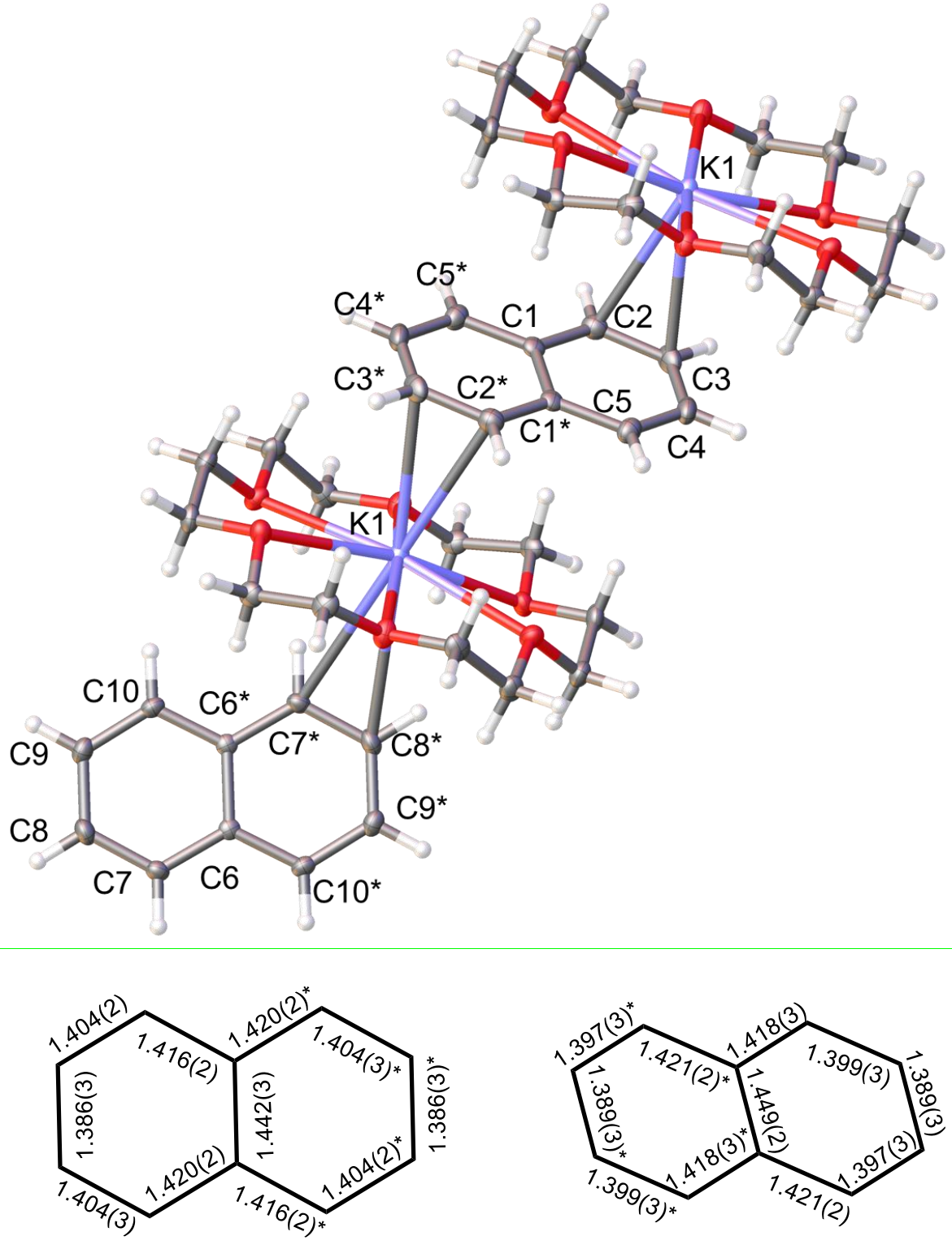

Figure S3. Solid-state molecular structure of **3** with 50% probability ellipsoids and respective bond length (Å) diagram. Asterisks denote symmetry generated atoms and bond lengths.

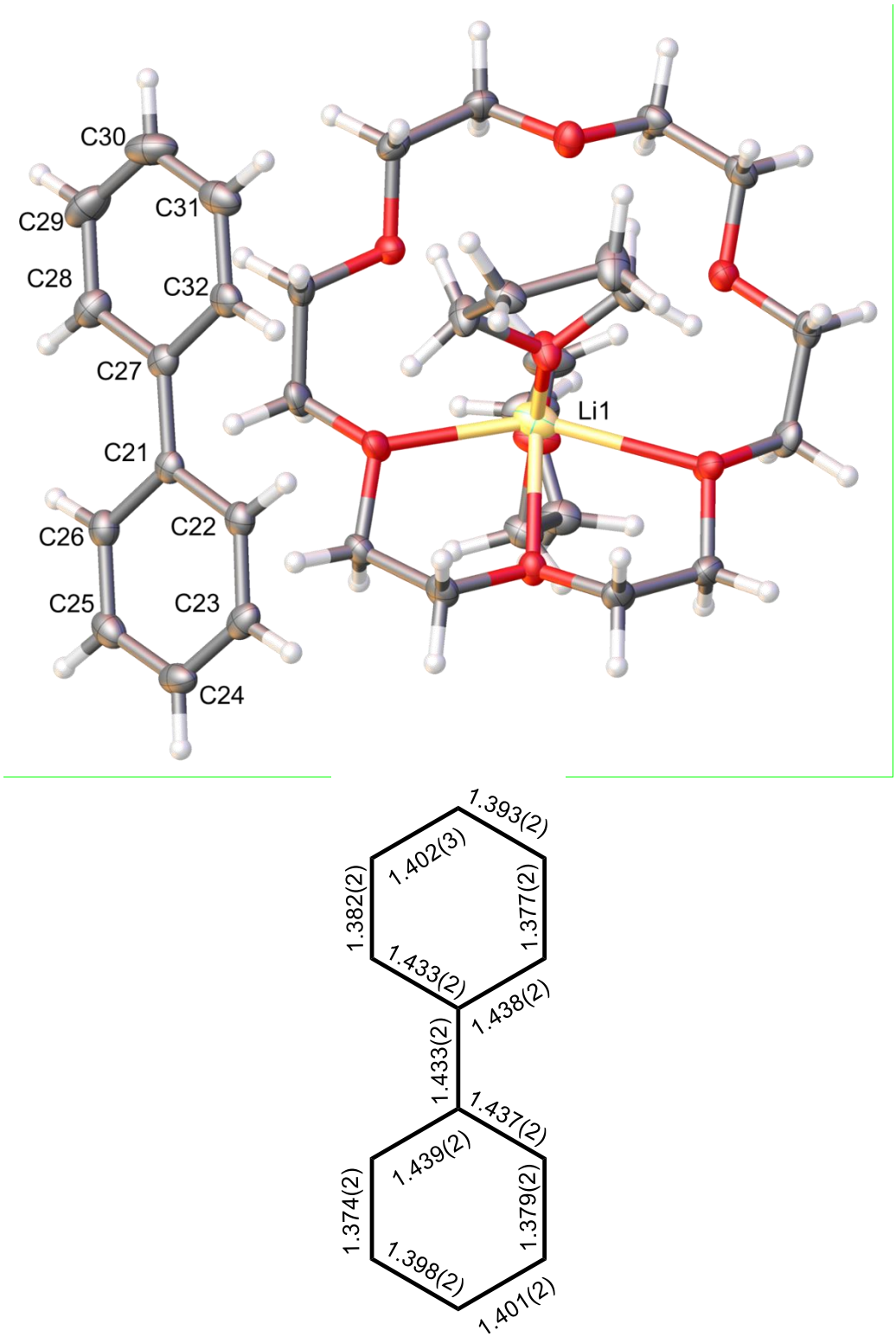

Figure S4. Solid-state molecular structure of **4** with 50% probability ellipsoids and respective bond length (Å) diagram. Asterisks denote symmetry generated atoms and bond lengths.

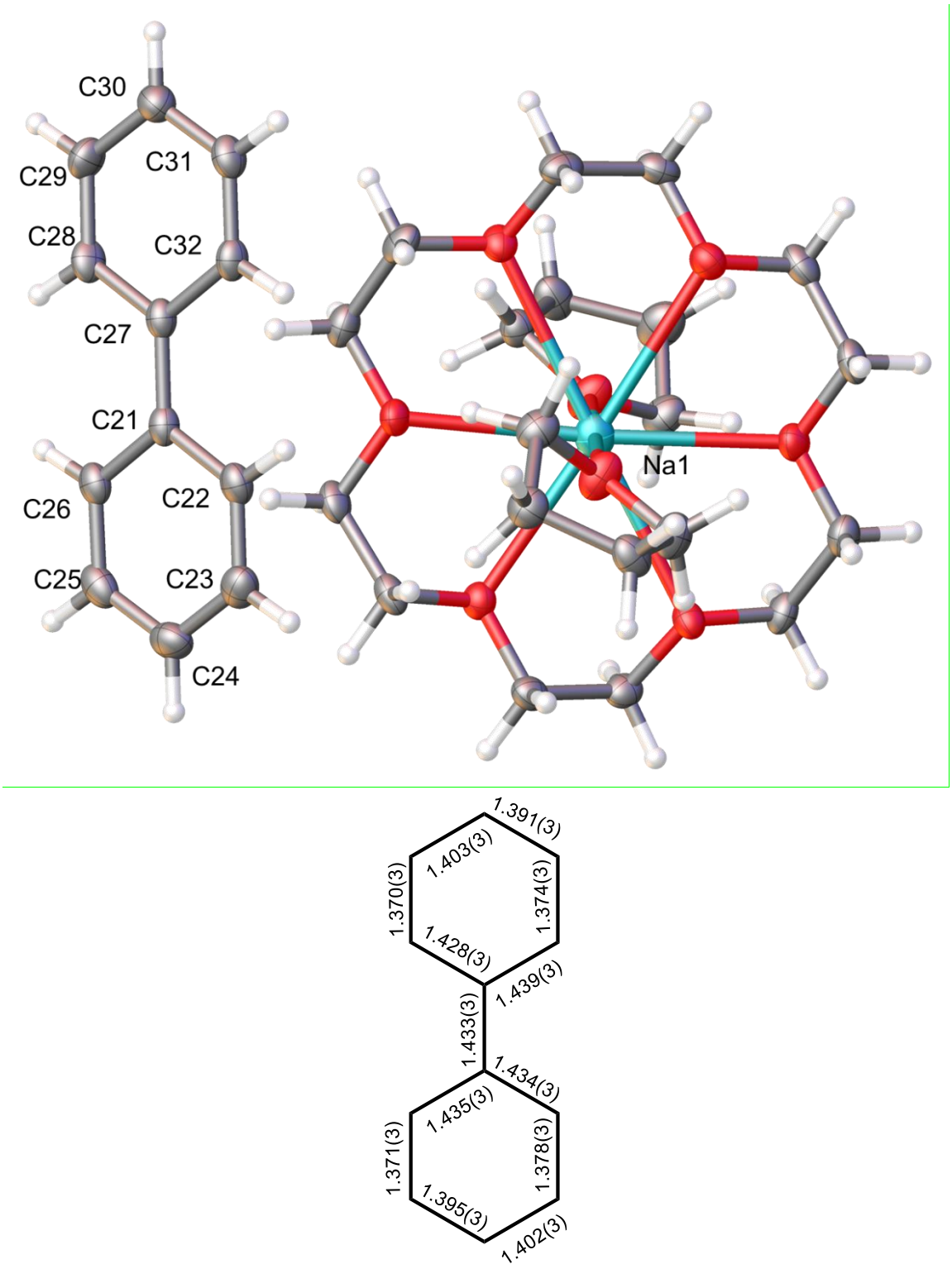

Figure S5. Solid-state molecular structure of **5** with 50% probability ellipsoids and respective bond length (Å) diagram.

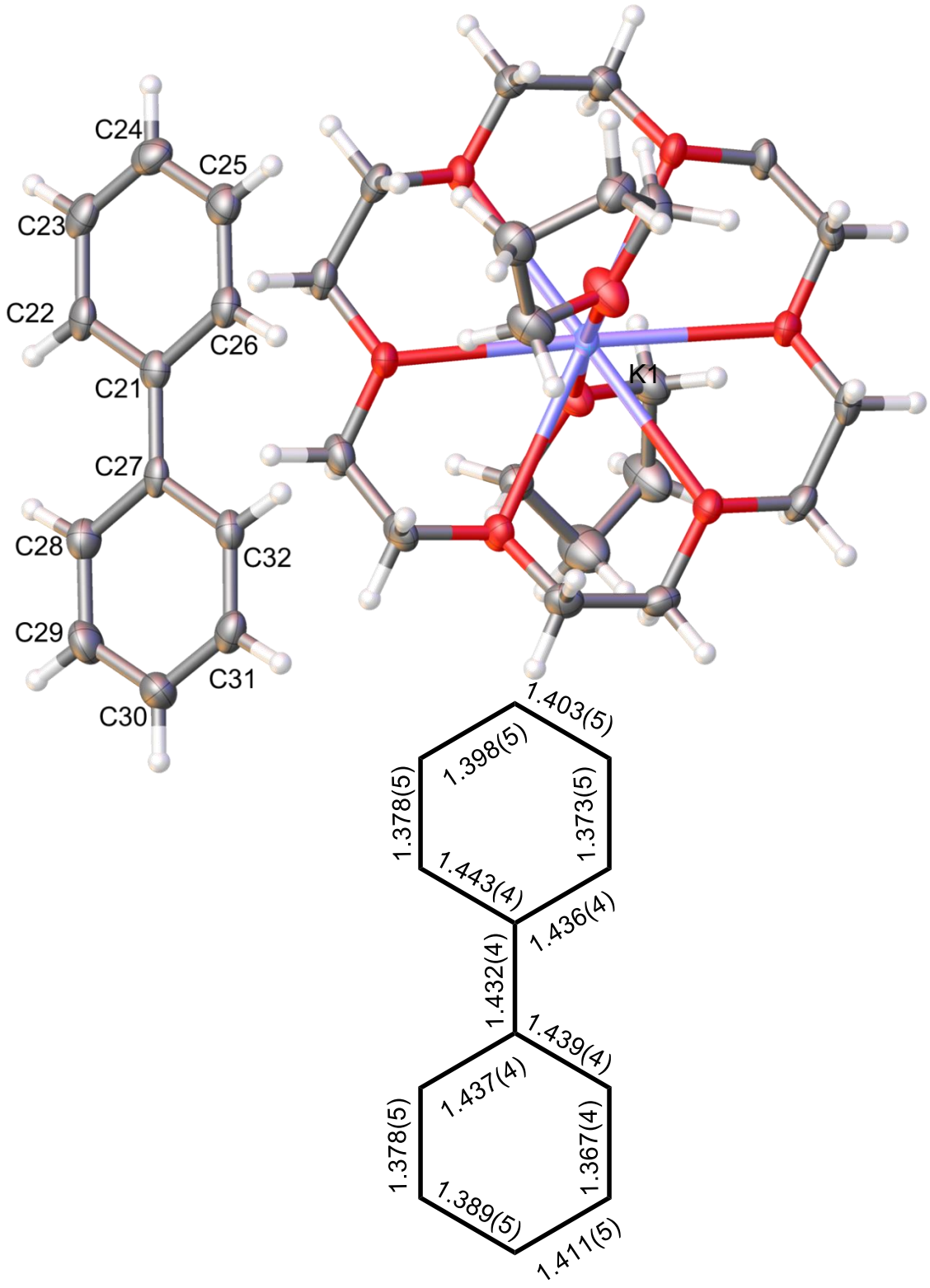

Figure S6. Solid-state molecular structure of **6** with 50% probability ellipsoids and respective bond length (Å) diagram.

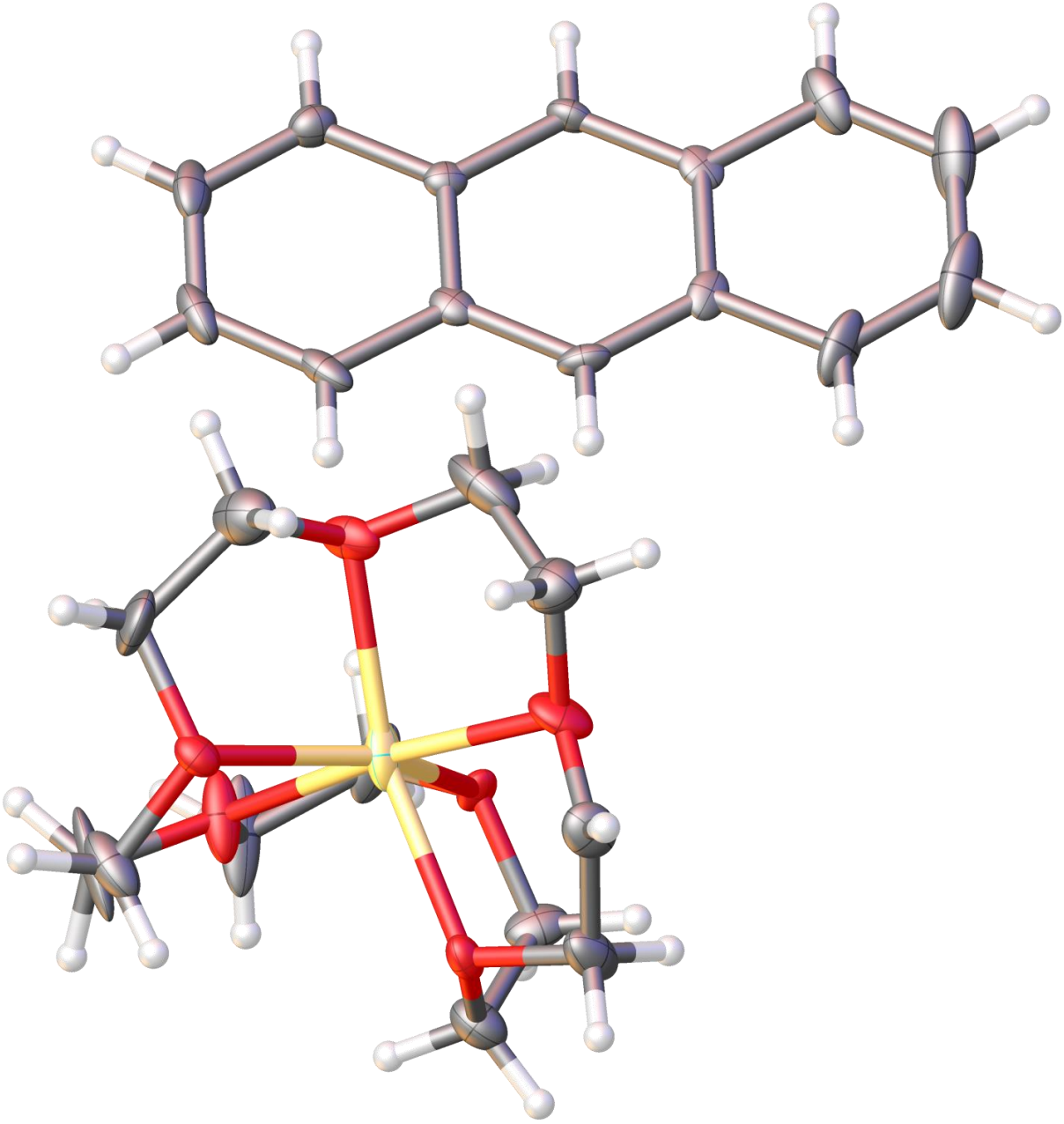

Figure S7. Diagram of the incompletely refined molecular structure of **7** presented to demonstrate connectivity only.

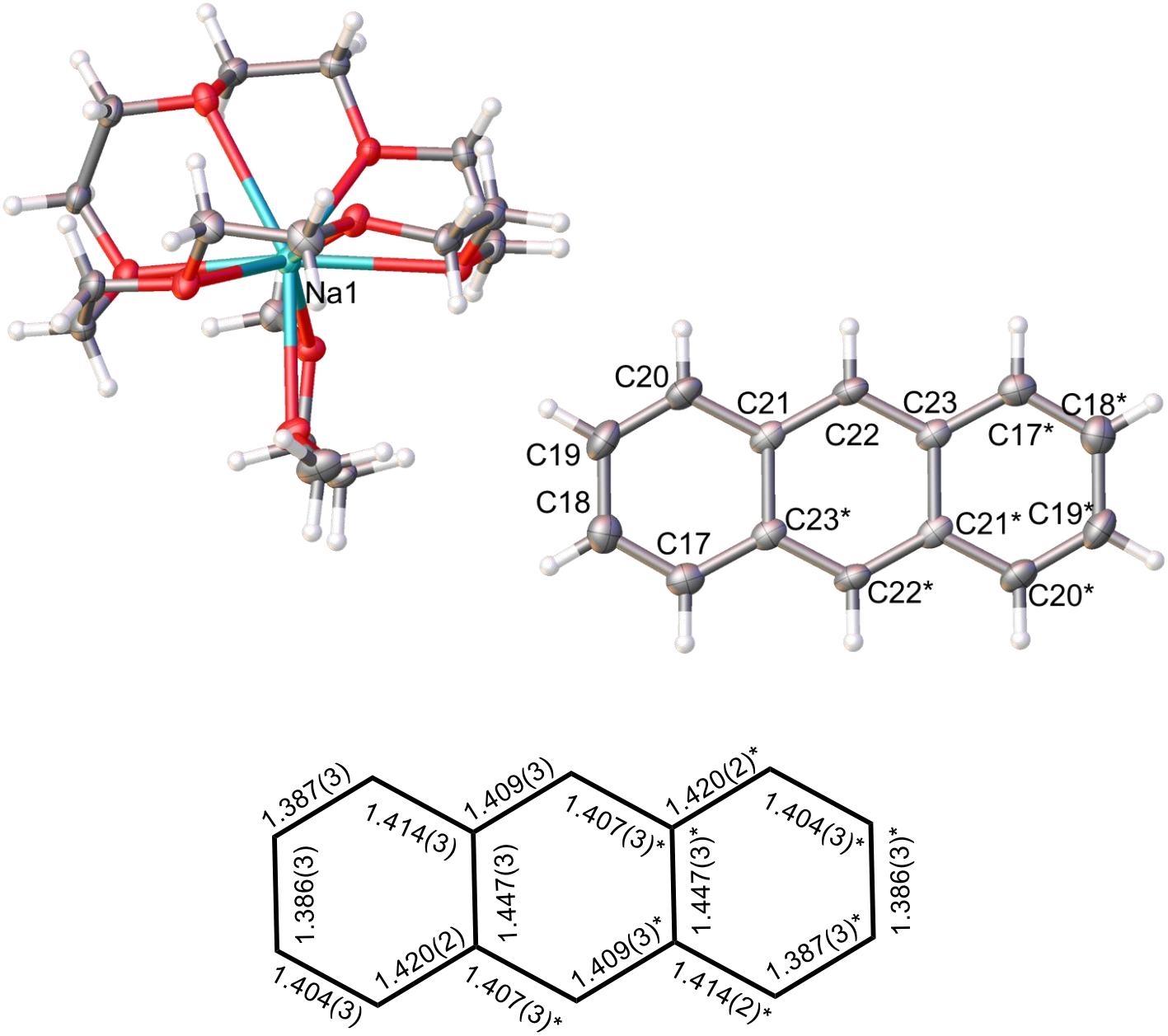

Figure S8. Solid-state molecular structure of **8** with 50% probability ellipsoids and respective bond length (Å) diagram. Asterisks denote symmetry generated atoms and bond lengths.

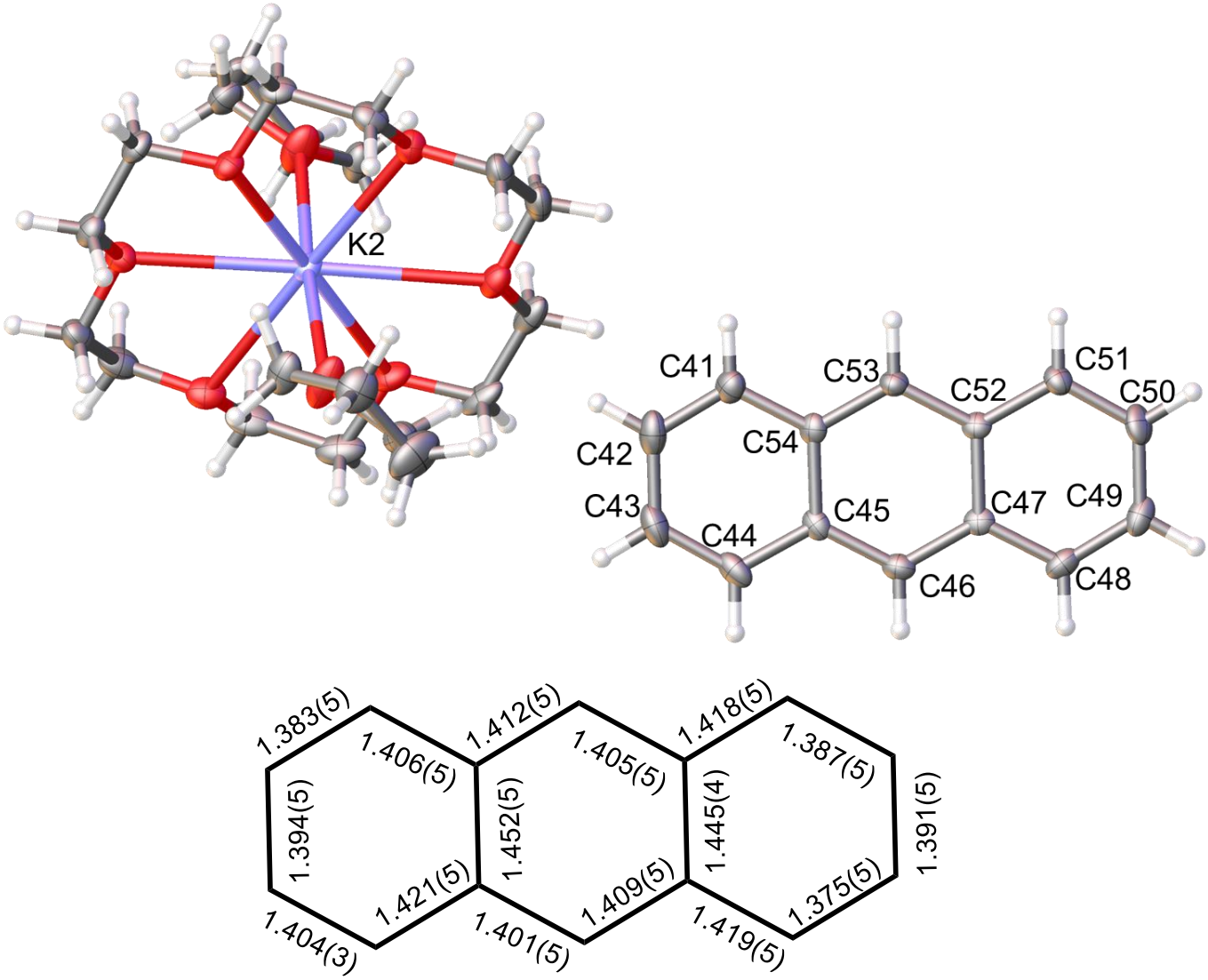

Figure S9. Solid-state molecular structure of **9** with 50% probability ellipsoids and respective bond length (Å) diagram.

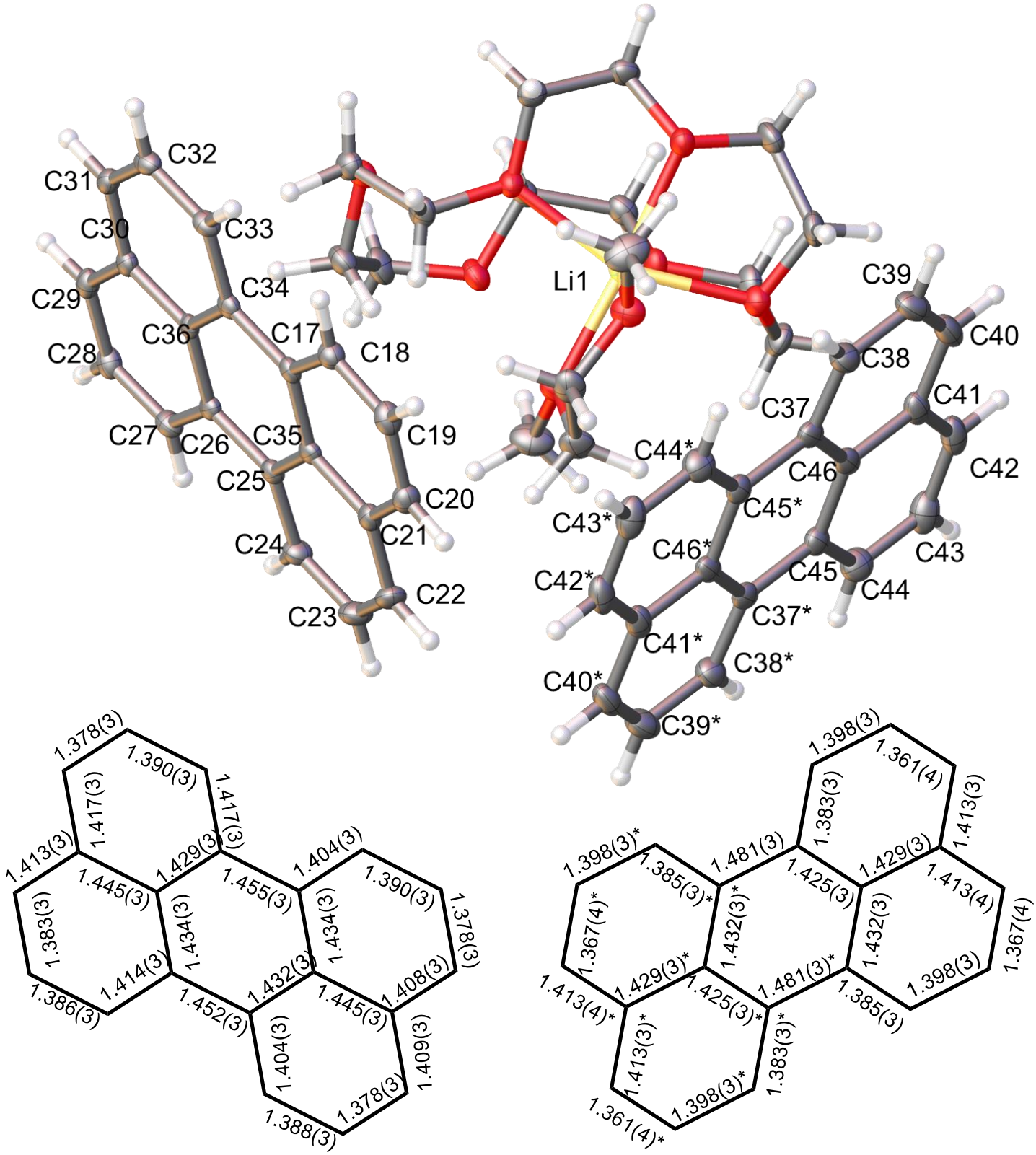

Figure S10. Solid-state molecular structure of **10** with 50% probability ellipsoids and respective bond length (Å) diagram. Asterisks denote symmetry generated atoms and bond lengths.

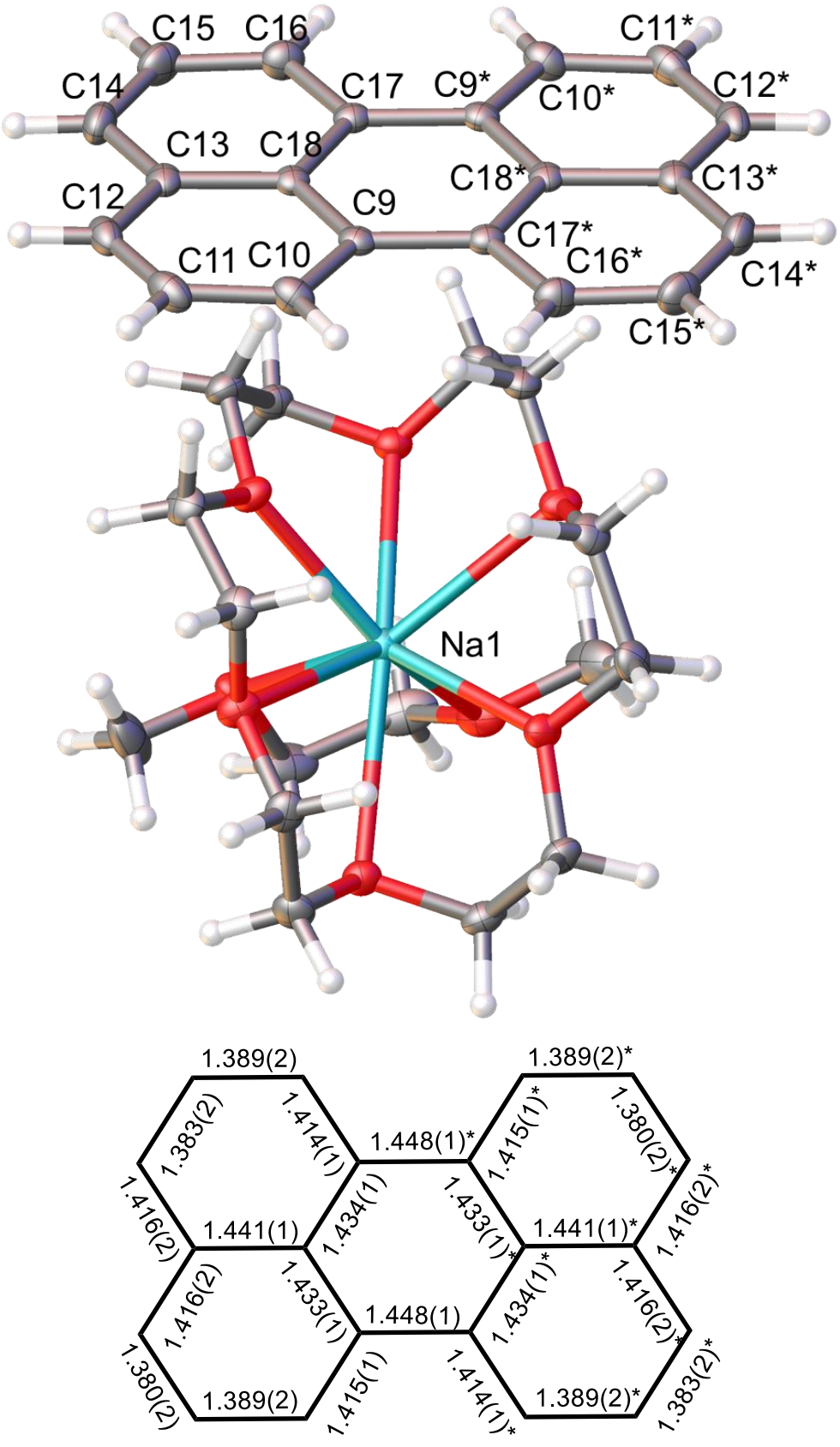

Figure S11. Solid-state molecular structure of **11** with 50% probability ellipsoids and respective bond length (Å) diagram. Asterisks denote symmetry generated atoms and bond lengths.

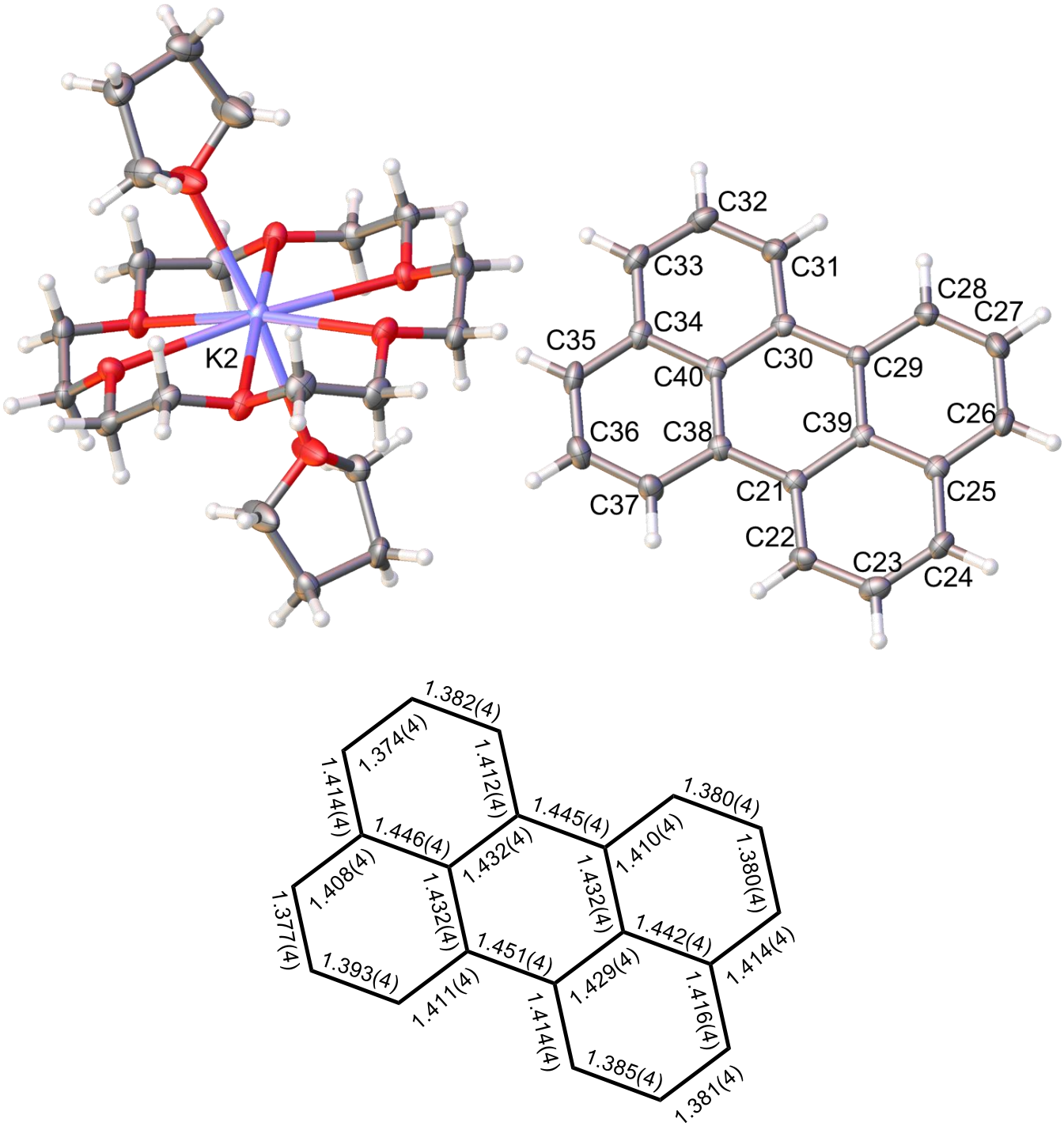

Figure S12. Solid-state molecular structure of **12** with 50% probability ellipsoids and respective bond length (Å) diagram.

Table S1. X-ray Crystallographic Data for Complexes **1-6** and **8-12**

	1	**2**	**3**	**4**
Empirical formula	$C_{22}H_{32}LiO_6$	$C_{26}H_{42}NaO_8$	$C_{22}H_{32}KO_6$	$C_{32}H_{50}LiO_8$
Crystal Habit, color	irregular, dark green	plate, dark green	block, dark green	rod, purple blue
Crystal size (mm)	0.10 × 0.08 × 0.05	0.4 × 0.3 × 0.05	0.27 × 0.13 × 0.11	0.90 × 0.37 × 0.15
Crystal system	orthorhombic	triclinic	triclinic	Monoclinic
Space group	*Pbca*	$P2_1/n$	$P\bar{1}$	$P2_1/c$
Volume ($Å^3$)	4186.1(3)	2646.3(4)	1109.0(2)	3151.2(4)
a (Å)	8.6020(3)	8.6161(8)	8.7069(8)	12.1048(8)
b (Å)	21.8870(8)	15.756(1)	9.1354(8)	17.611(1)
c (Å)	22.2344(8)	19.686(2)	15.410(1)	15.213(1)
α(°)	90	90	98.506(2)	90
β(°)	90	98.022(2)	91.665(2)	103.670(1)
γ(°)	90	90	113.205(1)	90
Z	8	4	2	4
Formula weight (g/mol)	399.42	505.59	431.57	569.66
Density (calculated) (Mg/m^3)	1.268	1.269	1.292	1.201
Absorption coefficient (mm^{-1})	0.090	0.106	0.274	0.084
F_{000}	1720.0	1092.0	462.0	1236.0
Total no. reflections	4827	6523	5873	7229
Unique reflections	3792	3999	4238	5349
Final R indices [$I > 2\sigma(I)$]	$R_1 = 0.0368$, $wR_2 = 0.0918$	$R_1 = 0.0368$, $wR_2 = 0.0918$	$R_1 = 0.0513$, $wR_2 = 0.1081$	$R_1 = 0.0406$, $wR_2 = 0.1030$
Largest diff. peak and hole ($e^-Å^{-3}$)	0.32 and -0.23	0.30 and -0.30	0.35 and -0.49	0.26 and -0.20
GOF	1.025	1.006	1.035	1.000

	5	**6**	**8**	**9**
Empirical formula	$C_{32}H_{50}NaO_8$	$C_{32}H_{50}KO_8$	$C_{30}H_{44}NaO_8$	$C_{34}H_{50}KO_8$
Crystal Habit, color	rod, purple blue	rod, purple	plate, purple	block, blue-purple
Crystal size (mm)	0.6 × 0.3 × 0.2	0.5 × 0.2 × 0.18	0.18 × 0.09 × 0.02	0.30 × 0.10 × 0.05
Crystal system	monoclinic	monoclinic	triclinic	monoclinic
Space group	$P2_1/n$	$P2_1/n$	$P\bar{1}$	$P2_1$
Volume ($Å^3$)	3176.1(6)	3244.5(5)	1484.90(15)	3359.0(4)
a (Å)	12.7772(13)	12.892(1)	11.5114(7)	13.0082(8)
b (Å)	17.6539(18)	18.017(2)	11.8386(7)	18.1719(11)
c (Å)	15.1994(15)	15.295(1)	13.6270(8)	15.3774(10)
α(°)	90	90	65.2130(10)	90
β(°)	112.120(2)	114.036(2)	70.1690(10)	112.4700(10)
γ(°)	90	90	63.7510(10)	90
Z	4	4	2	4
Formula weight (g/mol)	585.71	599.80	555.64	625.84
Density (calculated) (Mg/m^3)	1.225	1.228	1.243	1.238
Absorption coefficient (mm^{-1})	0.098	0.211	0.101	0.206
F_{000}	1268.0	1292.0	598.0	1348.0
Total no. reflections	4798	7460	6810	14982
Unique reflections	3149	4130	4442	11167
Final R indices [$I > 2\sigma(I)$]	$R_1 = 0.0424$, $wR_2 = 0.1110$	$R_1 = 0.0607$, $wR_2 = 0.1708$	$R_1 = 0.0491$, $wR_2 = 0.1074$	$R_1 = 0.0444$, $wR_2 = 0.0878$
Largest diff. peak and hole ($e^-Å^{-3}$)	0.21 and -0.23	0.76 and -0.43	0.25 and -0.27	0.33 and -0.26
GOF	1.004	1.020	1.011	1.004

	10	**11**	**12**
Empirical formula	$C_{46}H_{52}LiO_8$	$C_{36}H_{46}NaO_8$	$C_{40}H_{52}KO_8$
Crystal Habit, color	block, purple	prism, purple	plate, dark purple
Crystal size (mm)	0.23 × 0.17 × 0.11	0.18 × 0.09 × 0.02	0.24 × 0.18 × 0.02
Crystal system	triclinic	monoclinic	monoclinic
Space group	$P\bar{1}$	C2/c	$P2_1/c$
Volume ($Å^3$)	1923.1(2)	3277.9(2)	7361.5(13)
a (Å)	8.3174(5)	22.1045(7)	17.5120(18)
b (Å)	12.2288(8)	12.5068(4)	18.3856(19)
c (Å)	20.1448(13)	16.0000(9)	23.115(2)
α(°)	104.2740(10)	90	90
β(°)	99.6340(10)	132.18	98.461(2)
γ(°)	97.9080(10)	90	90
Z	2	4	8
Formula weight (g/mol)	739.81	629.72	699.91
Density (calculated) (Mg/m^3)	1.278	1.276	1.263
Absorption coefficient (mm^{-1})	0.086	0.100	0.196
F_{000}	790.0	1348.0	3000.0
Total no. reflections	9534	3809	18221
Unique reflections	5153	3414	11429
Final R indices [$I > 2\sigma(I)$]	$R_1 = 0.0635$, $wR_2 = 0.1438$	$R_1 = 0.0335$, $wR_2 = 0.0954$	$R_1 = 0.0656$, $wR_2 = 0.1784$
Largest diff. peak and hole ($e^-Å^{-3}$)	0.33 and -0.25	0.38 and -0.21	0.84 and -0.46
GOF	0.976	1.024	1.040

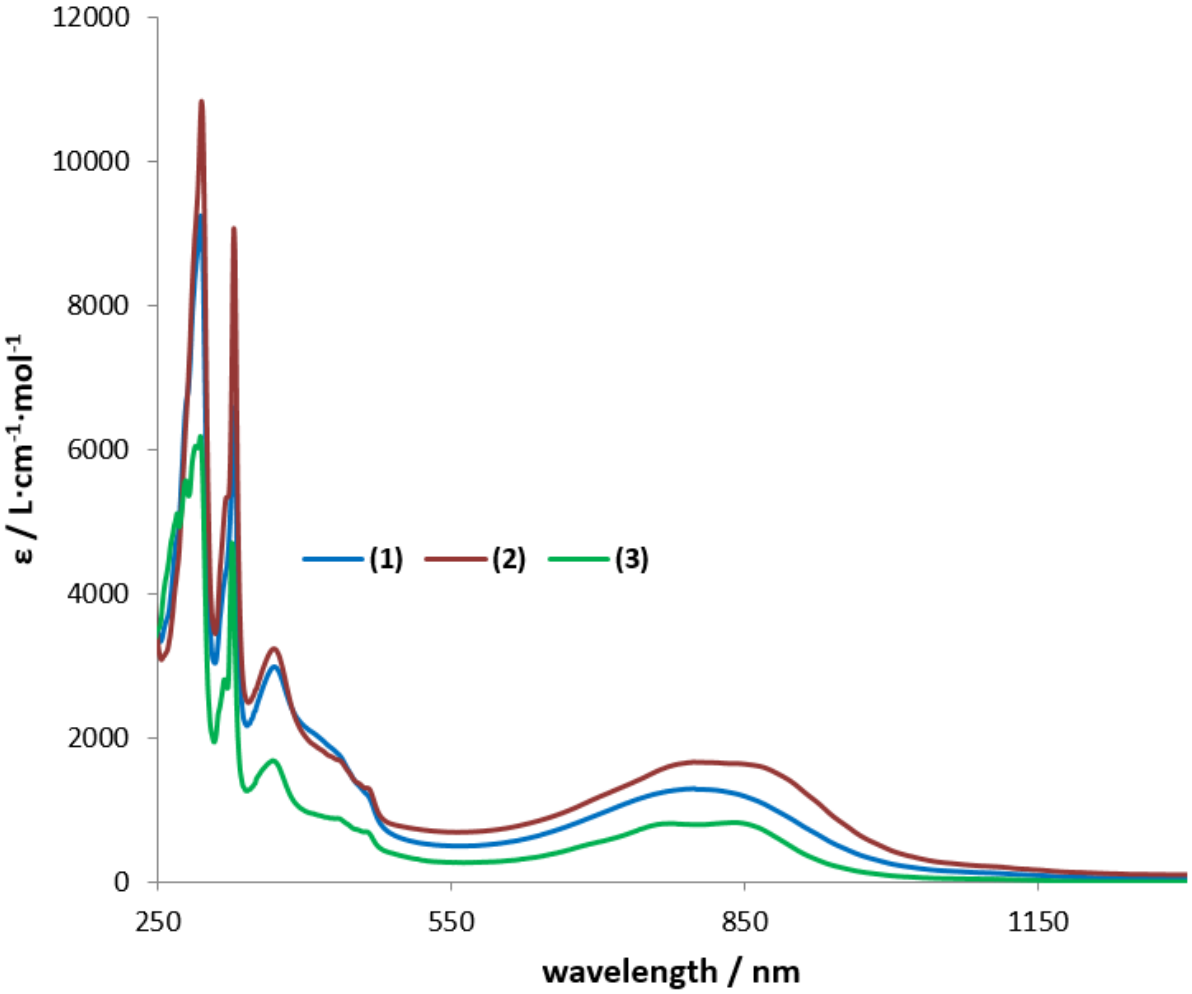

Figure S13. Room temperature UV/vis-NIR absorption spectra for **1** (THF, 0.106 mM), **2** (THF, 0.139 mM), and **3** (THF, 0.114 mM).

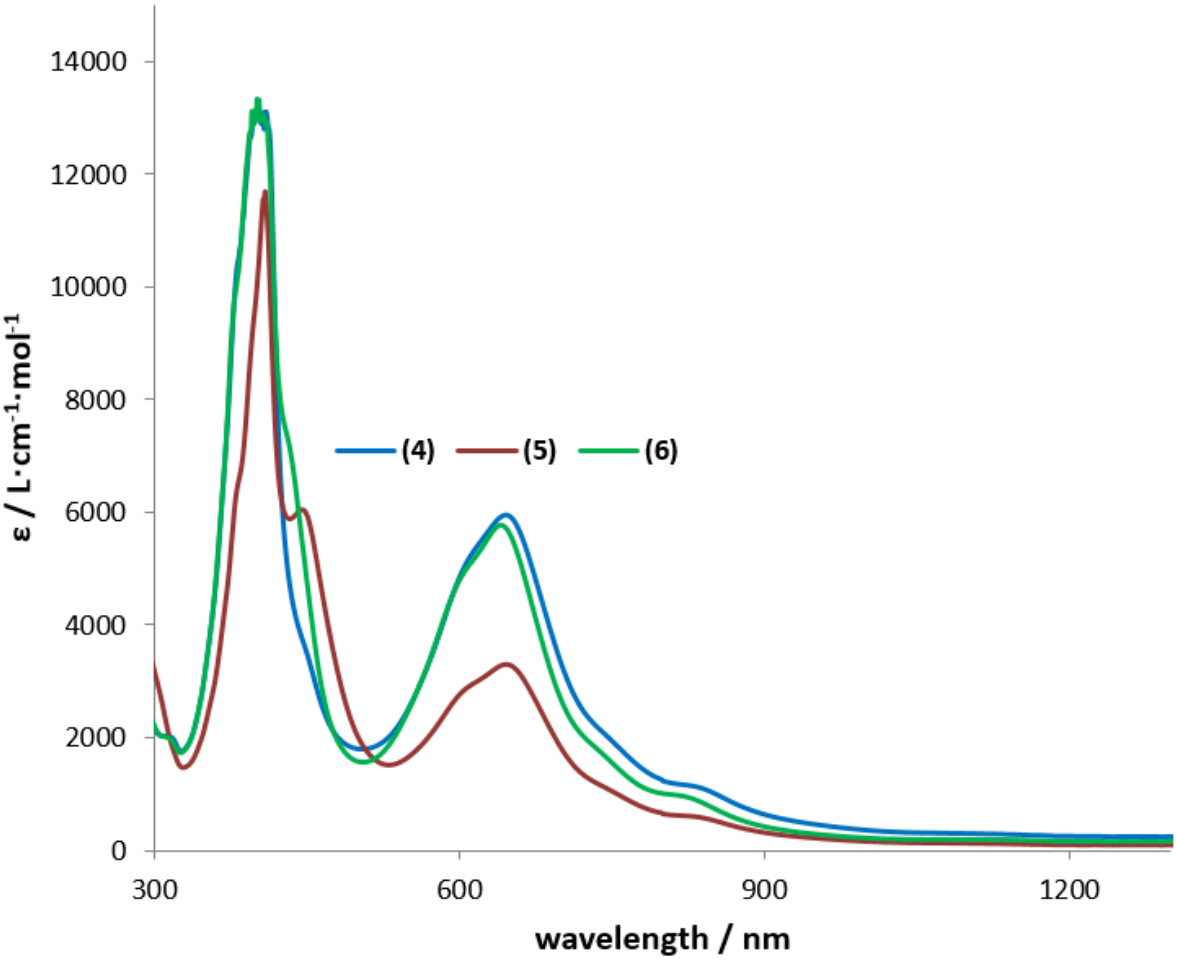

Figure S14. Room temperature UV/vis-NIR absorption spectra for **4** (THF, 0.284 mM), **5** (THF, 0.284 mM), and **6** (THF, 0.284 mM).

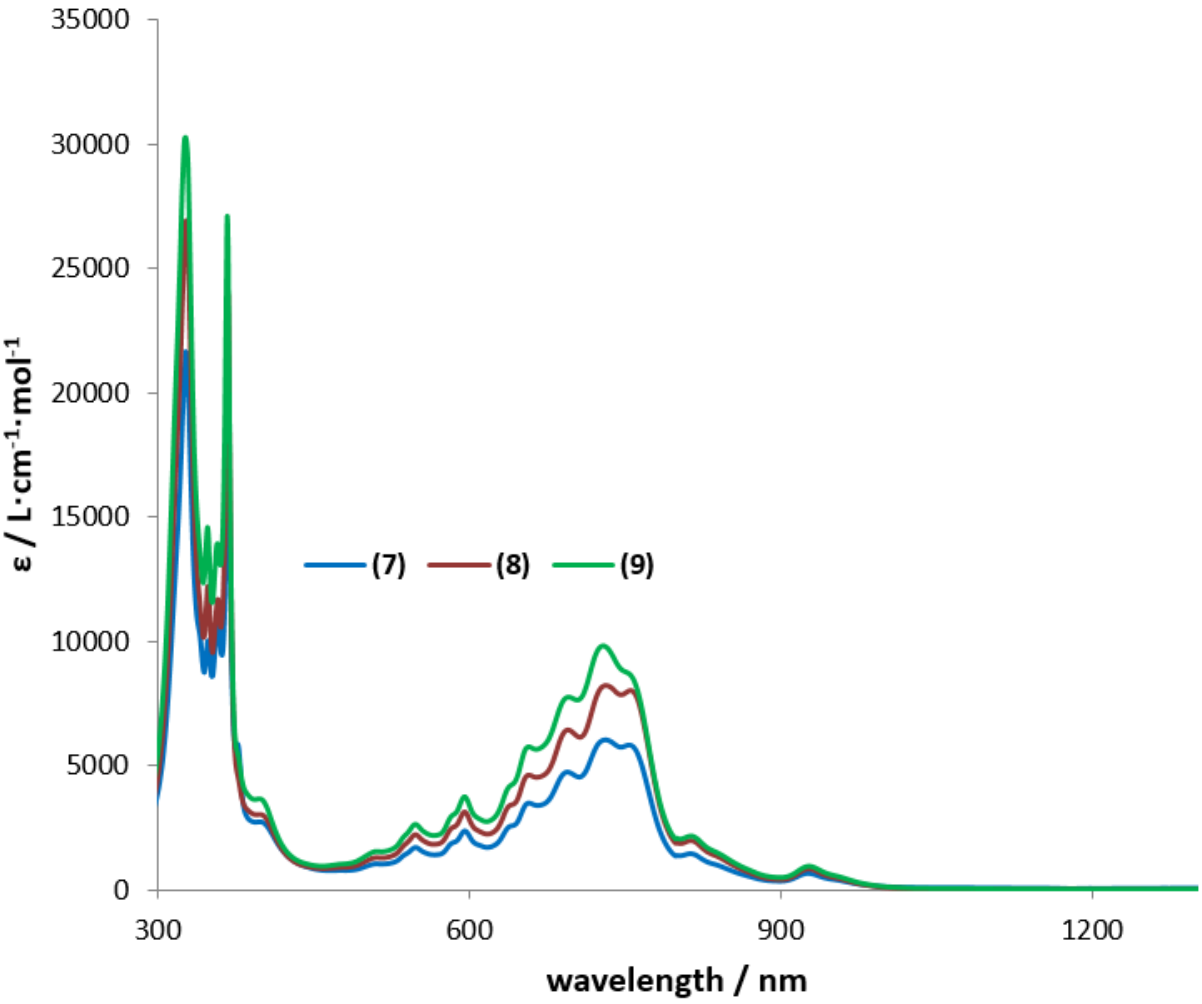

Figure S15. Room temperature UV/vis-NIR absorption spectra for **7** (THF, 0.105 mM), **8** (THF, 0.115 mM), and **9** (THF, 0.116 mM).

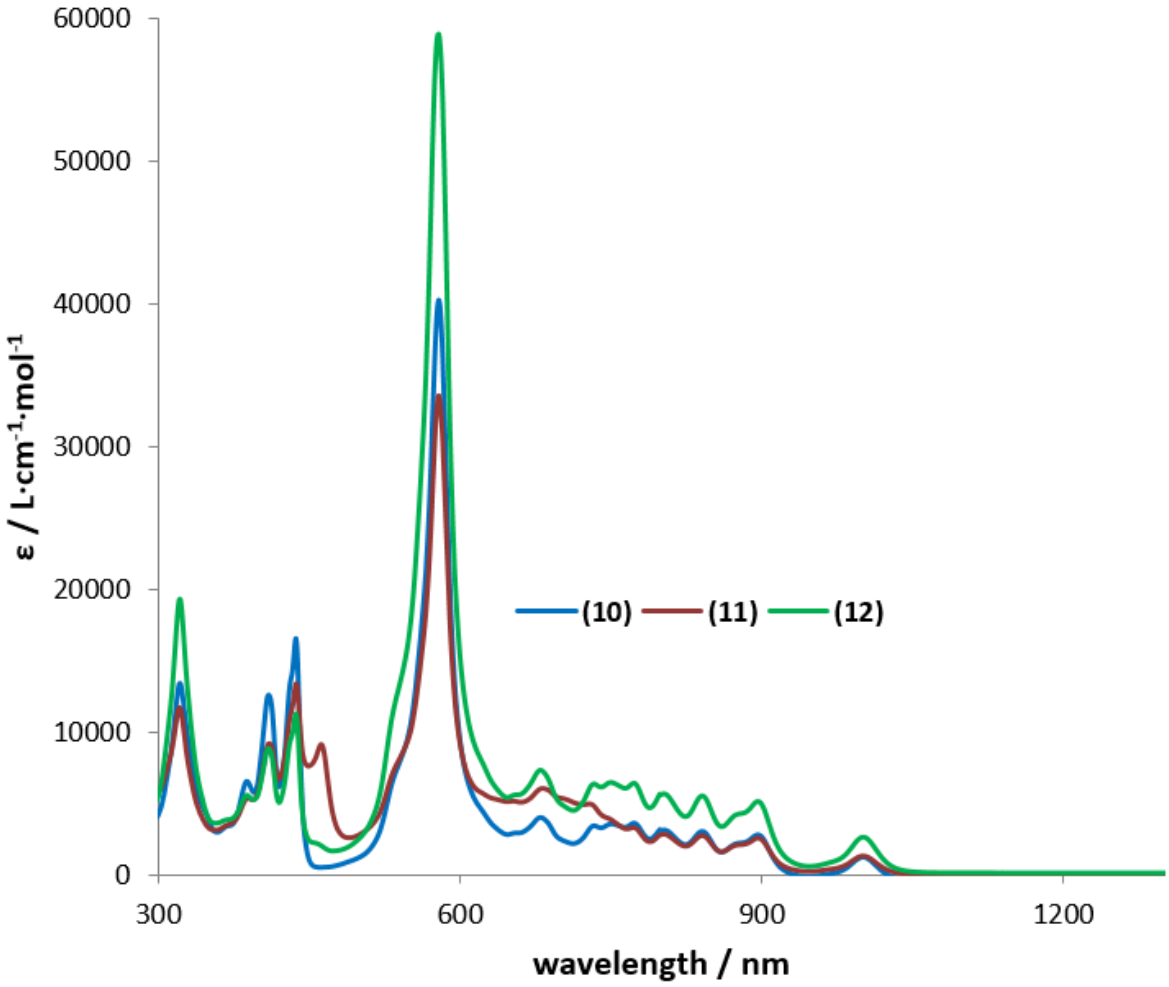

Figure S16. Room temperature UV/vis-NIR absorption spectra for **10** (THF, 0.036 mM), **11** (THF, 0.052 mM), and **12** (THF, 0.054 mM).

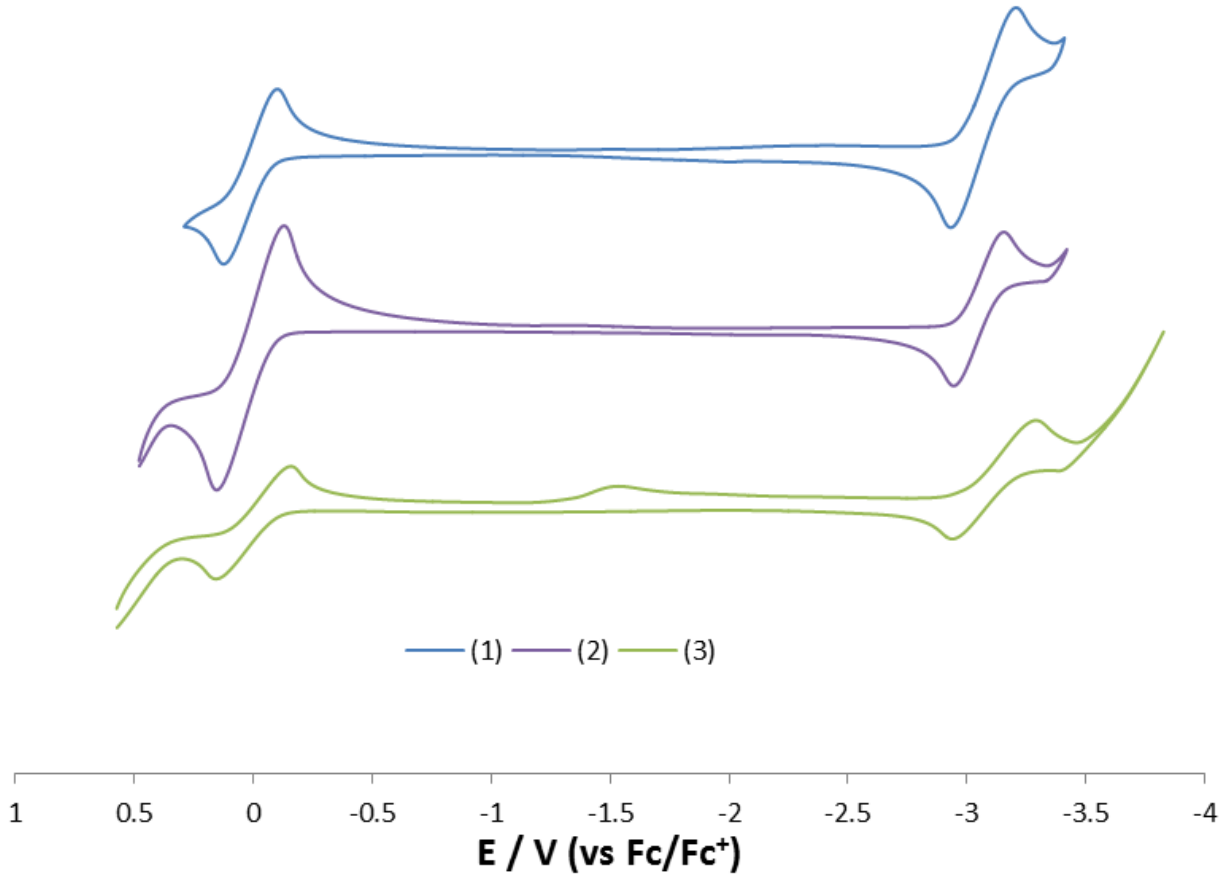

Figure S17. Room temperature cyclic voltammogram of **1**, **2** and **3** in DME (50 mV/s scan rate) vs internally referenced Cp_2Fe/Cp_2Fe^+ at $E_{1/2}$=0 V. (0.1M $[NBu_4][PF_6]$ as supporting electrolyte).

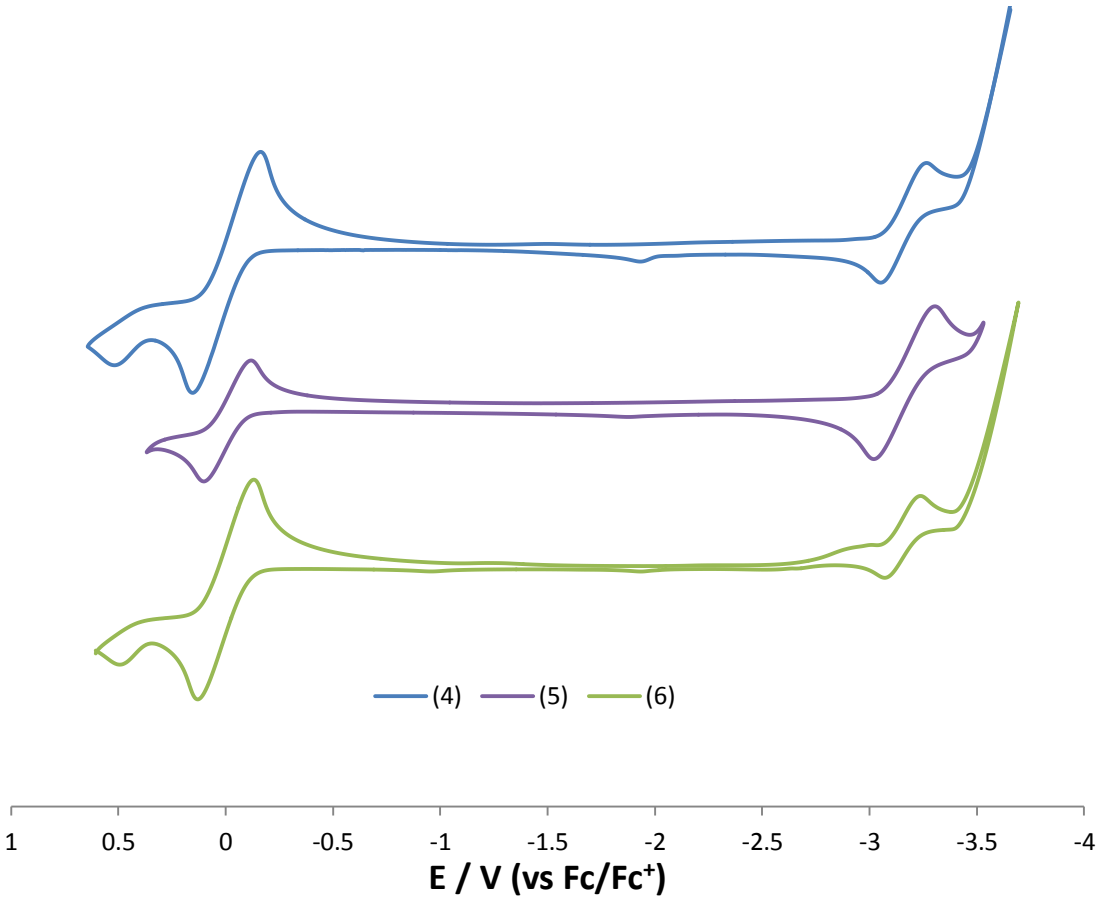

Figure S18. Room temperature cyclic voltammogram of **4** (50 mV/s scan rate), **5** (200 mV/s scan rate) and **6** (50 mV/s scan rate) in DME vs internally referenced Cp_2Fe/Cp_2Fe^+ at $E_{1/2}$=0. (0.1M $[NBu_4][PF_6]$ as supporting electrolyte).

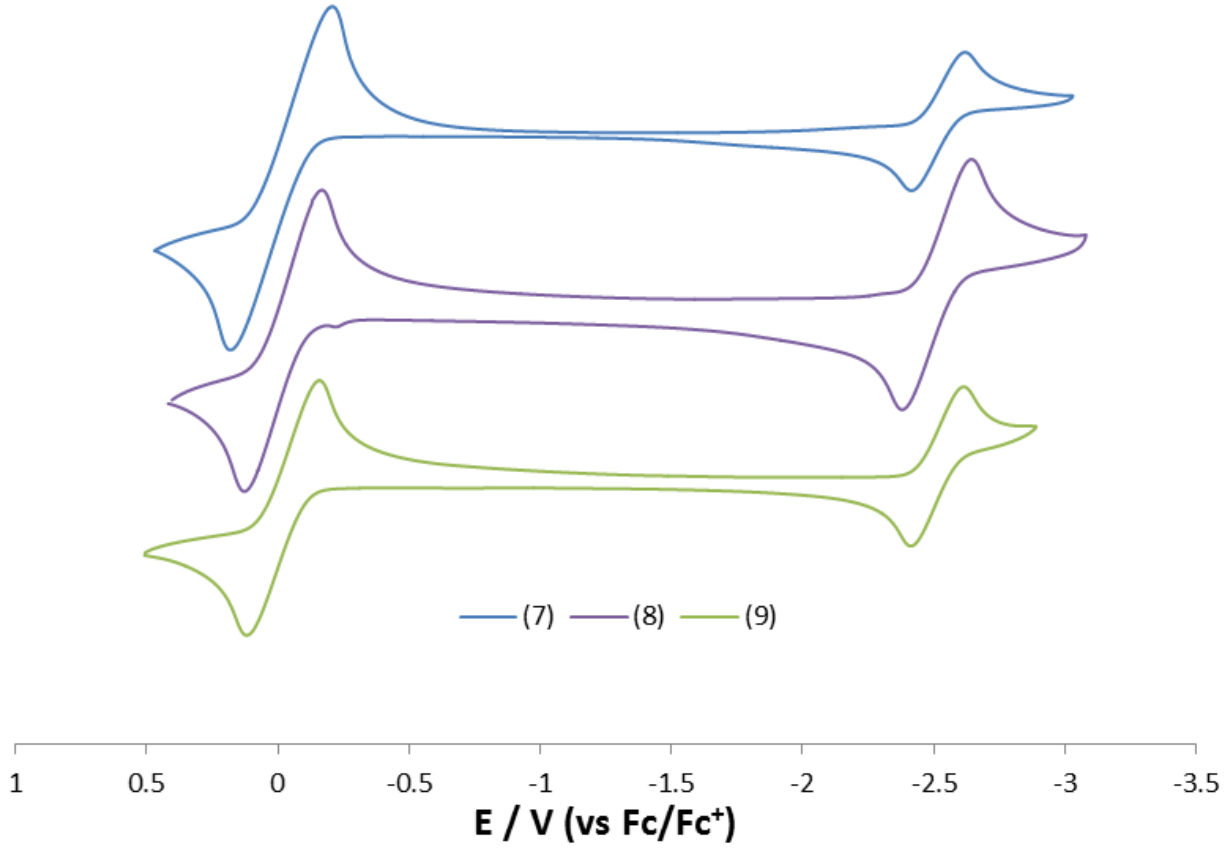

Figure S19. Room temperature cyclic voltammogram of **7** (50 mV/s scan rate), **8** (300 mV/s scan rate) and **9** (200 mV/s scan rate) in DME vs internally referenced Cp_2Fe/Cp_2Fe^+ at $E_{1/2}$=0 V. (0.1M $[NBu_4][PF_6]$ as supporting electrolyte).

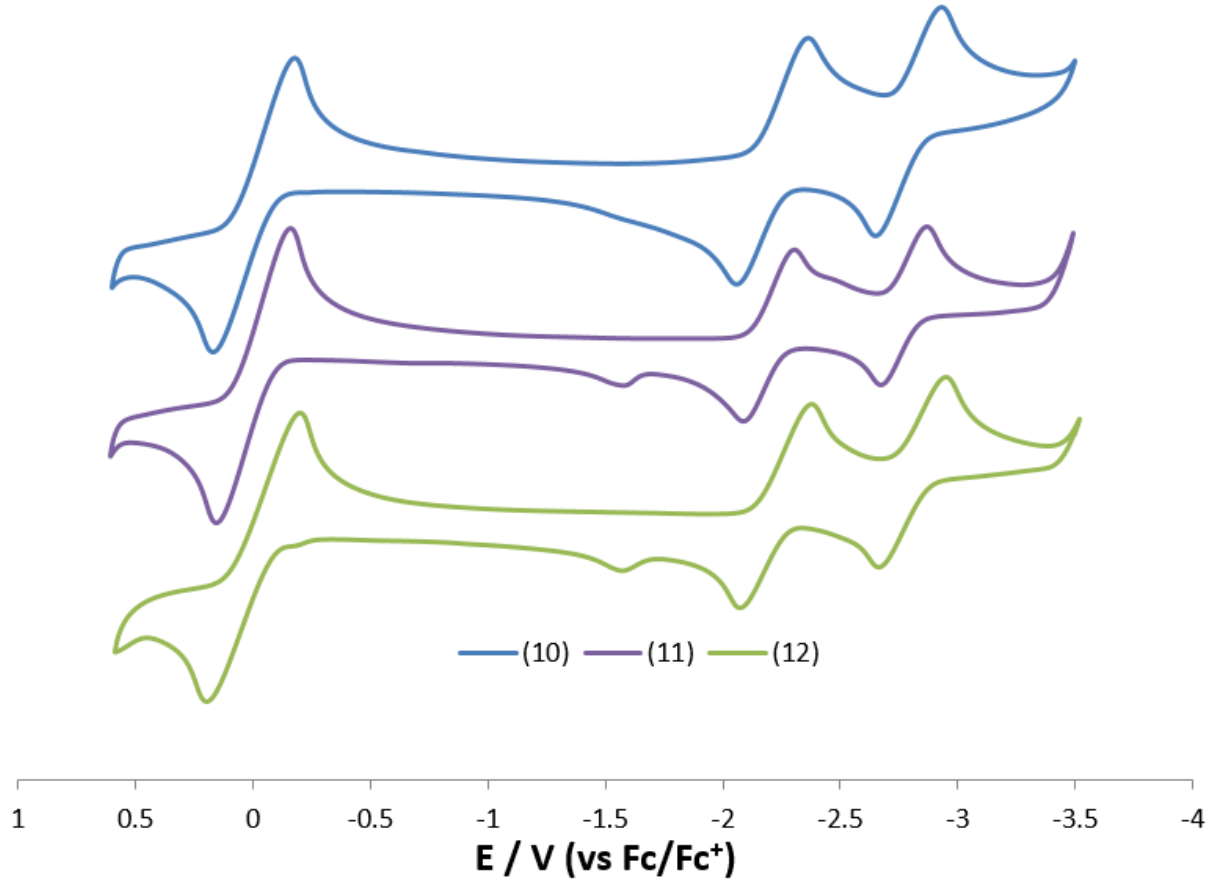

Figure S20. Room temperature cyclic voltammogram of **10**, **11** and **12** in DME (200mV/s scan rate) vs internally referenced Cp_2Fe/Cp_2Fe^+ at $E_{1/2}$=0 V. (0.1M $[NBu_4][PF_6]$ as supporting electrolyte).

Figure S21. Room temperature cyclic voltammogram of **1** in DME (vs internally referenced Cp_2Fe/Cp_2Fe^+ at $E_{1/2}$=0 V). (0.1M $[NBu_4][PF_6]$ as supporting electrolyte).

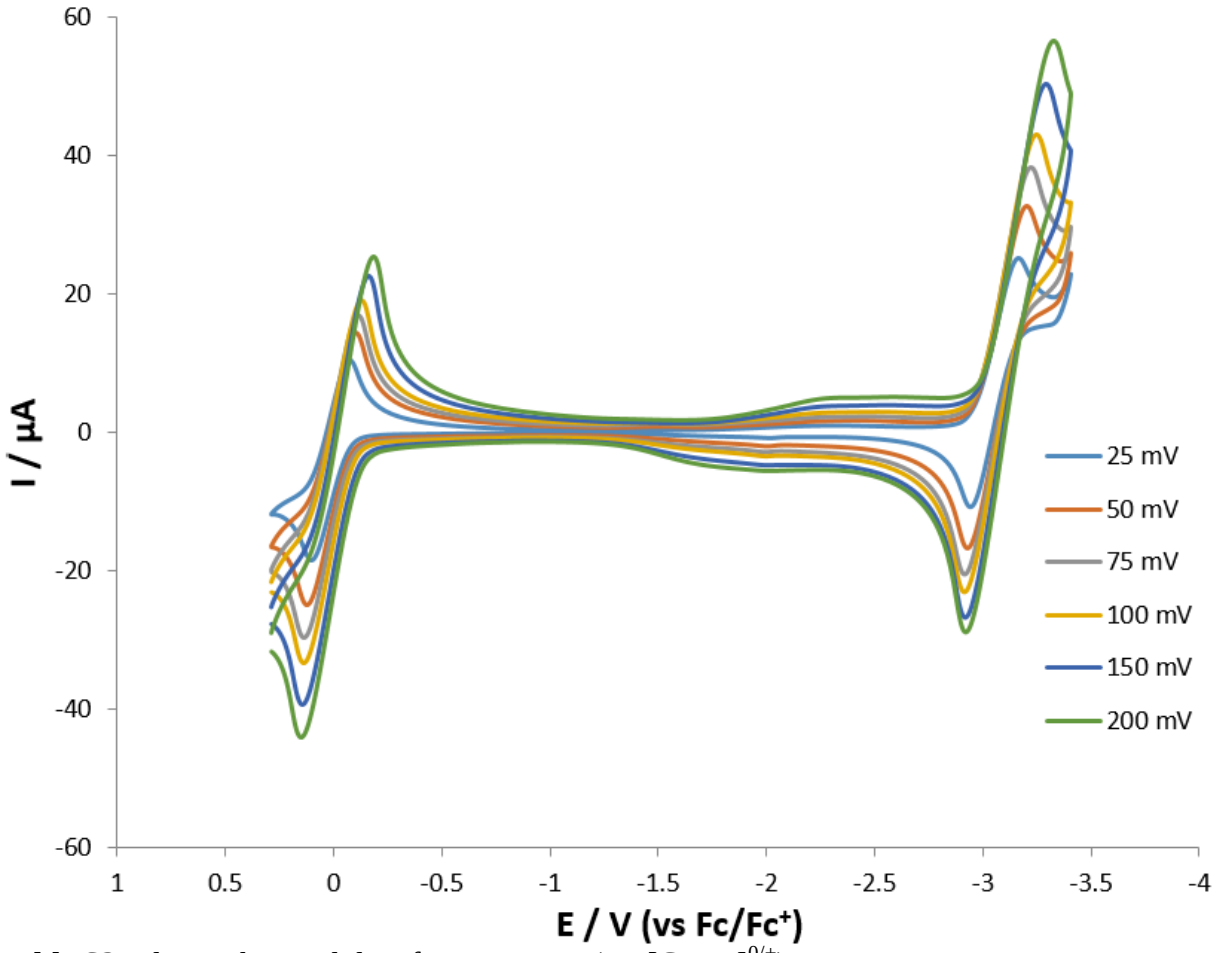

Table S2. Electrochemical data for **1** in DME (vs. $[Cp_2Fe]^{0/+}$).

Feature 1	**Scan rate, V/s**	**$E_{p,c}$, V**	**$E_{p,a}$, V**	**ΔE_p, V**	**$i_{p,c}/i_{p,a}$**
	0.025	-3.17	-2.945	0.223	-0.90
	0.050	-3.21	-2.932	0.274	-1.01
	0.075	-3.23	-2.919	0.307	-1.08
	0.100	-3.25	-2.918	0.333	-1.13
	0.150	-3.30	-2.921	0.375	-1.42
	0.200	-3.33	-2.924	0.407	-1.92

Figure S22. Room temperature cyclic voltammogram of **2** in DME (vs internally referenced Cp_2Fe/Cp_2Fe^+ at $E_{1/2}$=0 V). (0.1M $[NBu_4][PF_6]$ as supporting electrolyte).

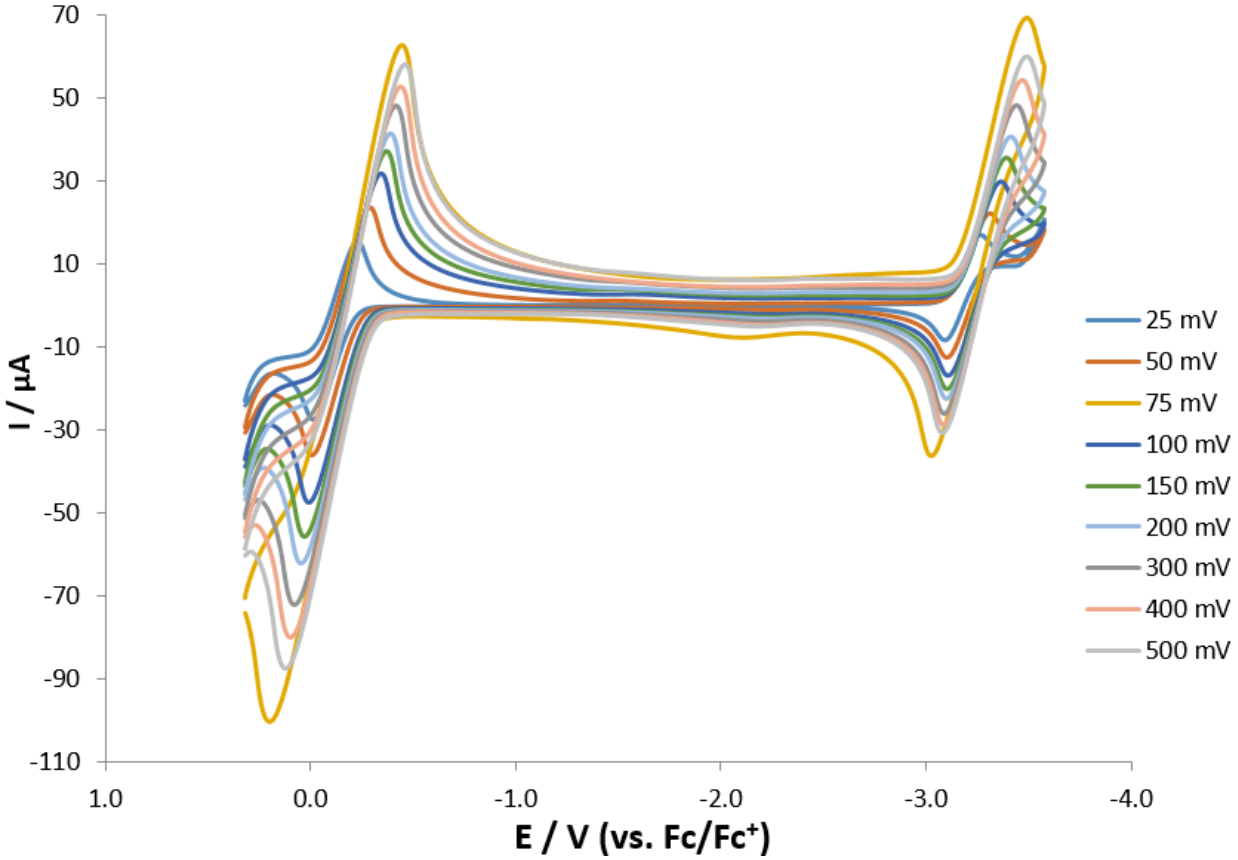

Table S3. Electrochemical data for **2** in DME (vs. $[Cp_2Fe]^{0/+}$).

Feature 1	**Scan rate, V/s**	**$E_{p,c}$, V**	**$E_{p,a}$, V**	**ΔE_p, V**	**$i_{p,c}/i_{p,a}$**
	0.025	-3.109	-2.934	0.175	0.95
	0.050	-3.155	-2.944	0.211	0.99
	0.075	-3.335	-2.868	0.467	2.08
	0.100	-3.208	-2.95	0.258	1.10
	0.150	-3.235	-2.946	0.289	1.15
	0.200	-3.257	-2.942	0.315	1.20
	0.300	-3.284	-2.931	0.353	1.33
	0.400	-3.312	-2.928	0.384	1.57
	0.500	-3.334	-2.922	0.412	1.96

Figure S23. Room temperature cyclic voltammogram of **3** in DME (vs internally referenced Cp_2Fe/Cp_2Fe^+ at $E_{1/2}$=0 V). (0.1M $[NBu_4][PF_6]$ as supporting electrolyte).

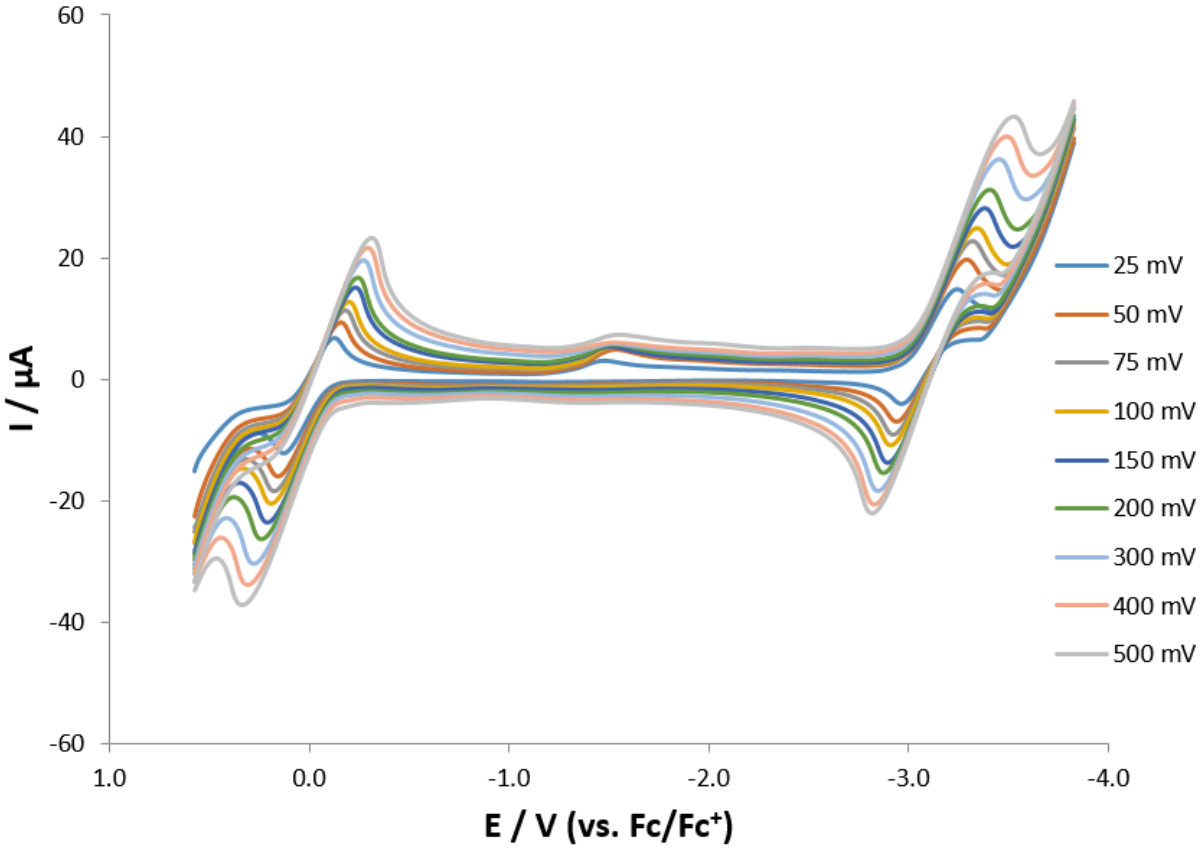

Table S4. Electrochemical data for **3** in DME (vs. $[Cp_2Fe]^{0/+}$).

Feature 1	**Scan rate, V/s**	**$E_{p,c}$, V**	**$E_{p,a}$, V**	**ΔE_p, V**	**$i_{p,c}/i_{p,a}$**
	0.025	-3.246	-2.967	0.279	0.94
	0.050	-3.294	-2.942	0.352	0.85
	0.075	-3.323	-2.925	0.398	0.82
	0.100	-3.246	-2.913	0.333	0.83
	0.150	-3.384	-2.898	0.486	0.85
	0.200	-3.409	-2.877	0.532	0.81
	0.300	-3.457	-2.85	0.607	0.84
	0.400	-3.493	-2.831	0.662	0.81
	0.500	-3.53	-2.821	0.709	1.01

Figure S24. Room temperature cyclic voltammogram of **4** in DME (vs internally referenced Cp_2Fe/Cp_2Fe^+ at $E_{1/2}$=0 V). (0.1M $[NBu_4][PF_6]$ as supporting electrolyte).

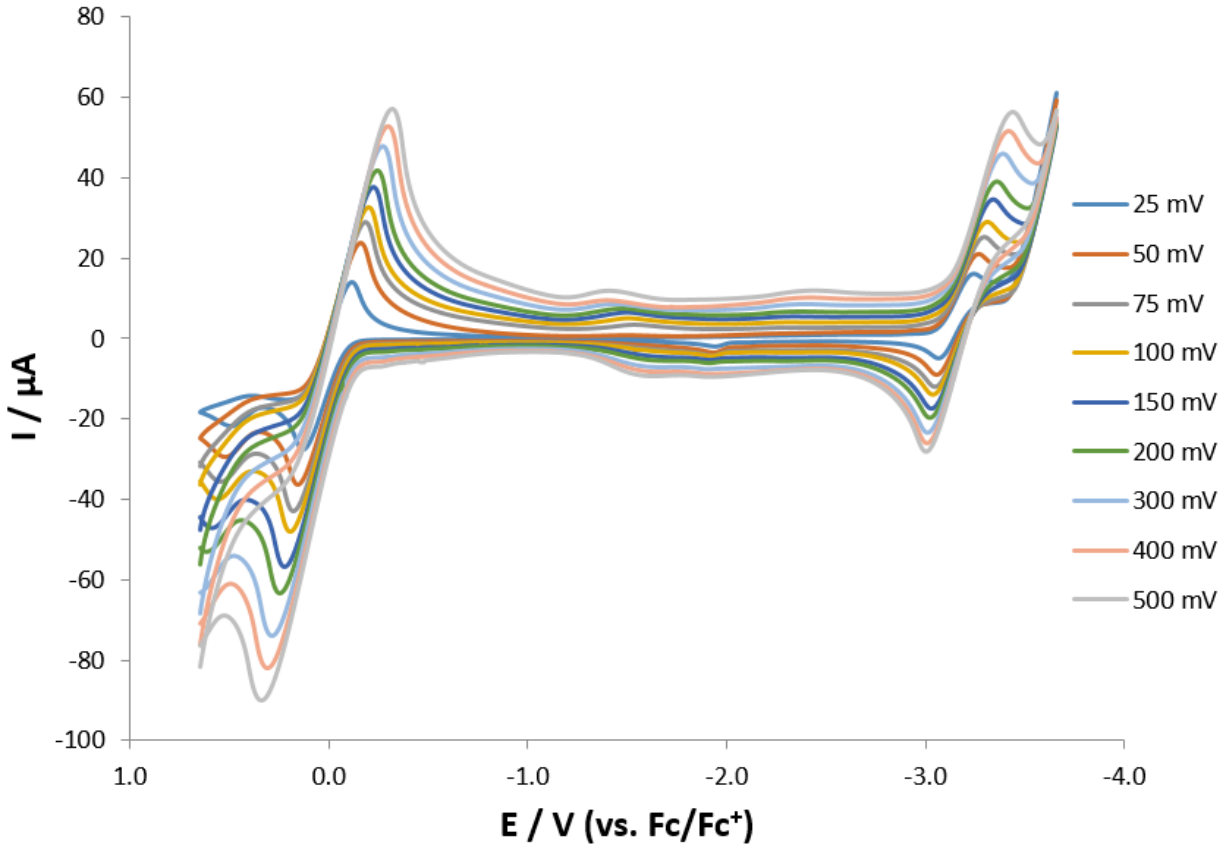

Table S5 Electrochemical data for **4** in DME (vs. $[Cp_2Fe]^{0/+}$).

Feature 1	**Scan rate, V/s**	**$E_{p,c}$, V**	**$E_{p,a}$, V**	**ΔE_p, V**	**$i_{p,c}/i_{p,a}$**
	0.025	-3.245	-3.067	0.178	1.09
	0.050	-3.269	-3.057	0.212	1.15
	0.075	-3.297	-3.049	0.248	1.05
	0.100	-3.313	-3.039	0.274	1.02
	0.150	-3.342	-3.032	0.31	1.08
	0.200	-3.36	-3.024	0.336	1.14
	0.300	-3.391	-3.012	0.379	1.20
	0.400	-3.42	-3.009	0.411	1.26
	0.500	-3.44	-3.005	0.435	1.28

Figure S25. Room temperature cyclic voltammogram of **5** in DME (vs internally referenced Cp_2Fe/Cp_2Fe^+ at $E_{1/2}$=0 V). (0.1M $[NBu_4][PF_6]$ as supporting electrolyte).

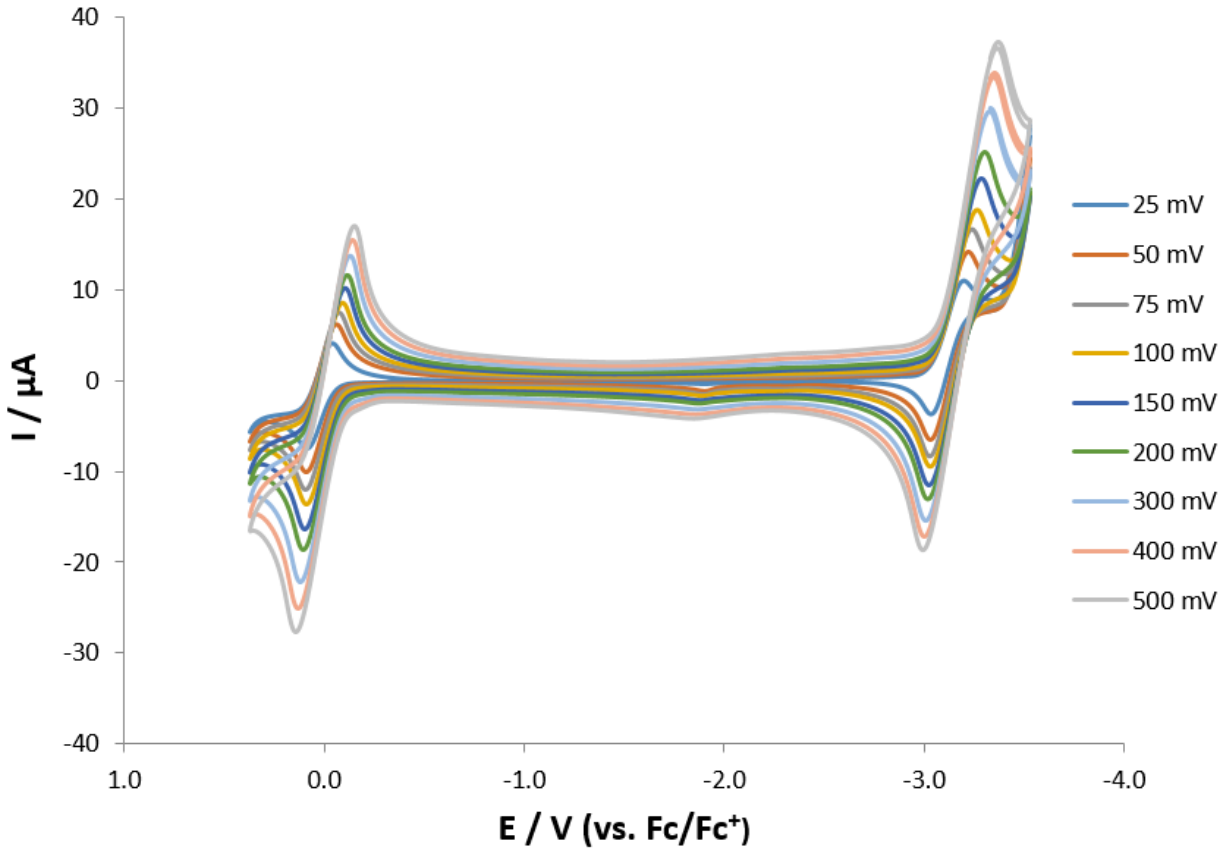

Table S6 Electrochemical data for **5** in DME (vs. $[Cp_2Fe]^{0/+}$).

Feature 1	**Scan rate, V/s**	**$E_{p,c}$, V**	**$E_{p,a}$, V**	**ΔE_p, V**	**$i_{p,c}/i_{p,a}$**
	0.025	-3.199	-3.035	0.164	0.69
	0.050	-3.221	-3.031	0.19	0.77
	0.075	-3.239	-3.028	0.211	0.85
	0.100	-3.265	-3.031	0.234	0.99
	0.150	-3.287	-3.024	0.263	1.19
	0.200	-3.303	-3.018	0.285	1.33
	0.300	-3.328	-3.008	0.32	1.18
	0.400	-3.348	-3.001	0.347	0.98
	0.500	-3.366	-2.994	0.372	1.04

Figure S26. Room temperature cyclic voltammogram of **6** in DME (vs internally referenced Cp_2Fe/Cp_2Fe^+ at $E_{1/2}$=0 V). (0.1M $[NBu_4][PF_6]$ as supporting electrolyte).

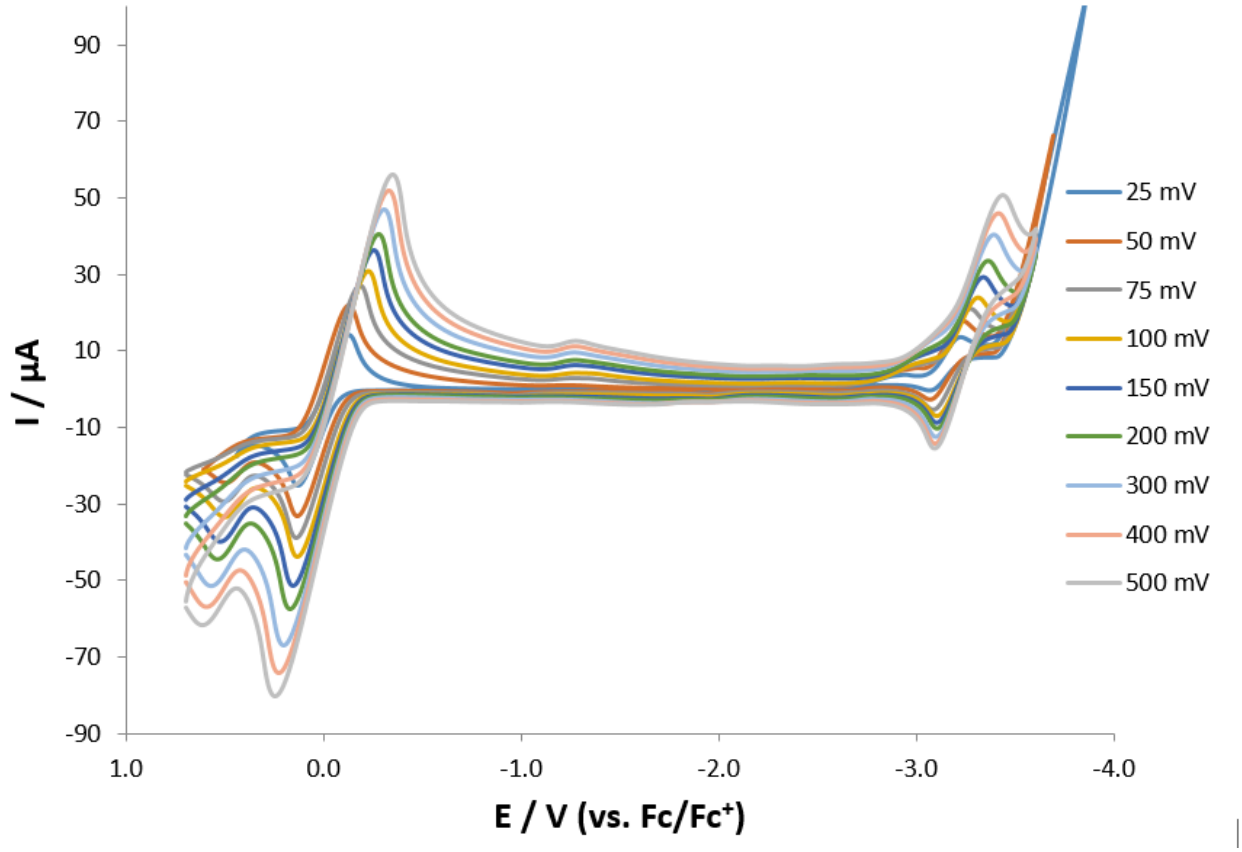

Table S7 Electrochemical data for **6** in DME (vs. $[Cp_2Fe]^{0/+}$).

Feature 1	**Scan rate, V/s**	**$E_{p,c}$, V**	**$E_{p,a}$, V**	**ΔE_p, V**	**$i_{p,c}/i_{p,a}$**
	0.025	-2.973	-2.814	0.159	1.34
	0.050	-3.153	-2.987	0.166	1.11
	0.075	-3.28	-3.09	0.19	0.85
	0.100	-3.318	-3.109	0.209	0.82
	0.150	-3.344	-3.108	0.236	0.78
	0.200	-3.369	-3.11	0.259	0.72
	0.300	-3.398	-3.104	0.294	0.69
	0.400	-3.421	-3.1	0.321	0.75
	0.500	-3.443	-3.098	0.345	0.87

Figure S27. Room temperature cyclic voltammogram of **7** in DME (vs internally referenced Cp_2Fe/Cp_2Fe^+ at $E_{1/2}$=0 V). (0.1M $[NBu_4][PF_6]$ as supporting electrolyte).

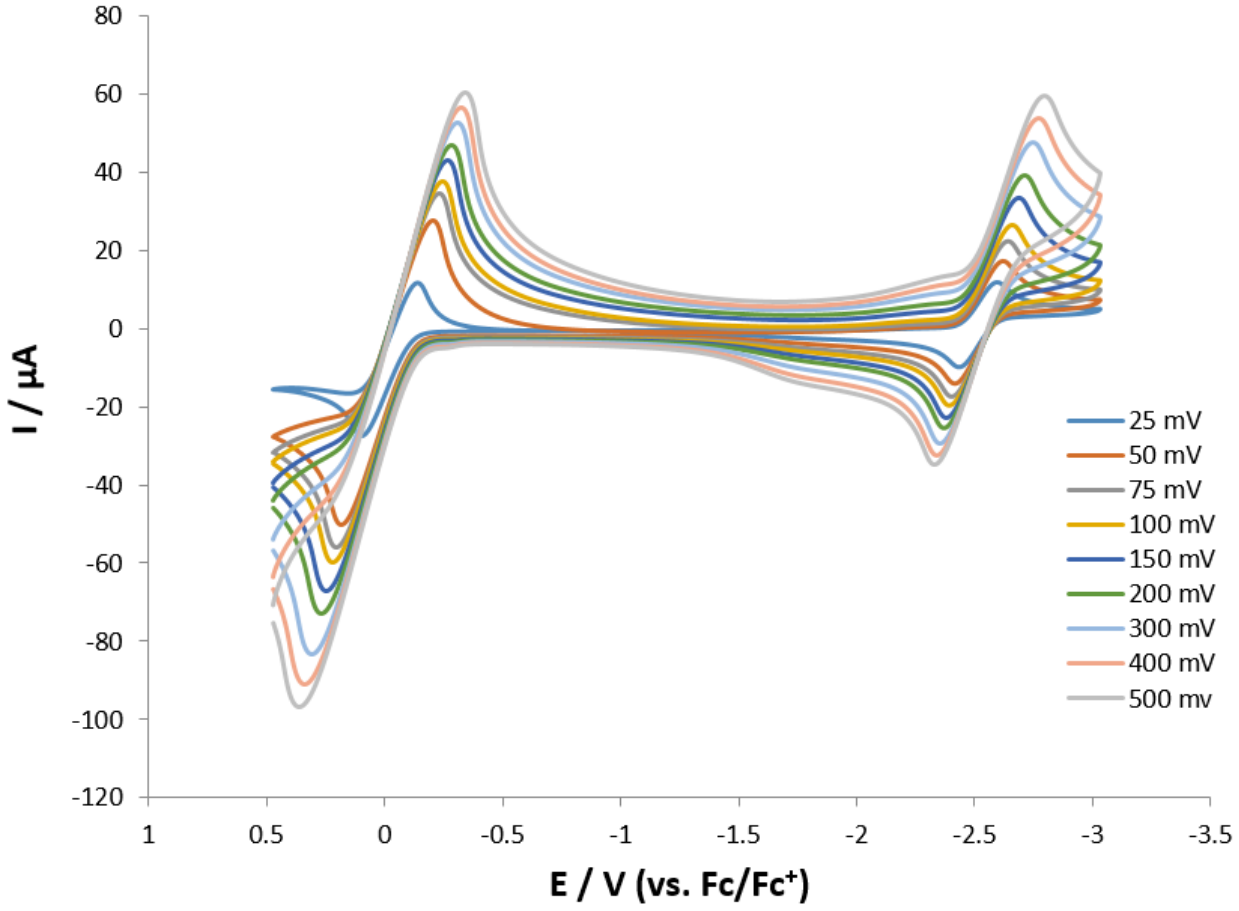

Table S8 Electrochemical data for **7** in DME (vs. $[Cp_2Fe]^{0/+}$).

Feature 1	**Scan rate, V/s**	**$E_{p,c}$, V**	**$E_{p,a}$, V**	**ΔE_p, V**	**$i_{p,c}/i_{p,a}$**
	0.025	-2.584	-2.423	0.161	0.94
	0.050	-2.609	-2.404	0.205	0.94
	0.075	-2.63	-2.391	0.239	0.96
	0.100	-2.648	-2.381	0.267	0.97
	0.150	-2.676	-2.368	0.308	0.99
	0.200	-2.7	-2.359	0.341	0.99
	0.300	-2.735	-2.342	0.393	1.00
	0.400	-2.76	-2.328	0.432	1.01
	0.500	-2.784	-2.319	0.465	1.02

Figure S28. Room temperature cyclic voltammogram of **8** in DME (vs internally referenced Cp_2Fe/Cp_2Fe^+ at $E_{1/2}$=0 V). (0.1M $[NBu_4][PF_6]$ as supporting electrolyte).

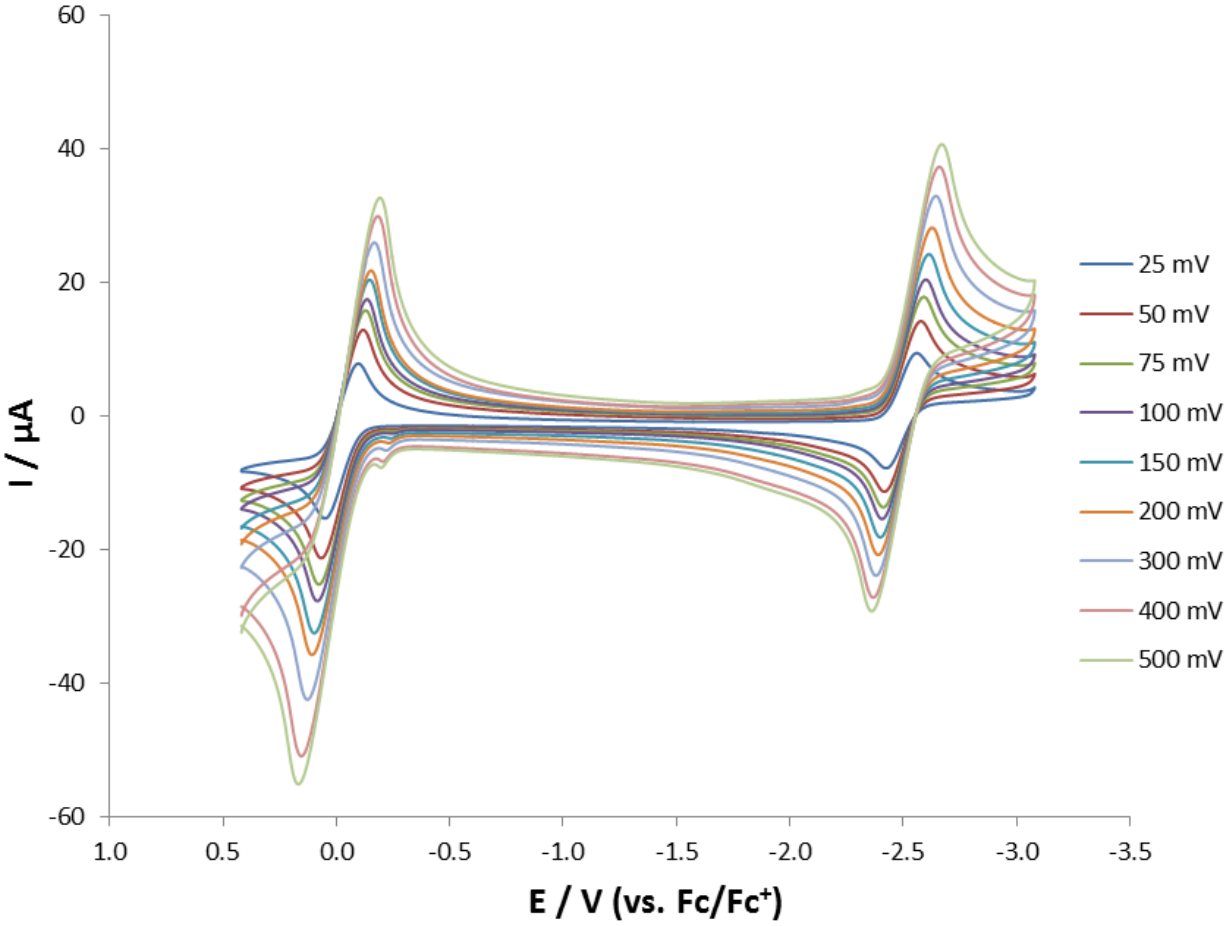

Table S9. Electrochemical data for **8** in DME (vs. $[Cp_2Fe]^{0/+}$).

Feature 1	**Scan rate, V/s**	**$E_{p,c}$, V**	**$E_{p,a}$, V**	**ΔE_p, V**	**$i_{p,c}/i_{p,a}$**
	0.025	-2.53	-2.394	0.136	1.08
	0.050	-2.548	-2.386	0.162	1.03
	0.075	-2.56	-2.381	0.179	1.03
	0.100	-2.569	-2.376	0.193	1.02
	0.150	-2.583	-2.368	0.215	1.04
	0.200	-2.597	-2.359	0.238	1.05
	0.300	-2.614	-2.349	0.265	1.38
	0.400	-2.629	-2.337	0.292	1.06
	0.500	-2.64	-2.33	0.31	1.38

Figure S29. Room temperature cyclic voltammogram of **9** in DME (vs internally referenced Cp_2Fe/Cp_2Fe^+ at $E_{1/2}$=0 V). (0.1M $[NBu_4][PF_6]$ as supporting electrolyte).

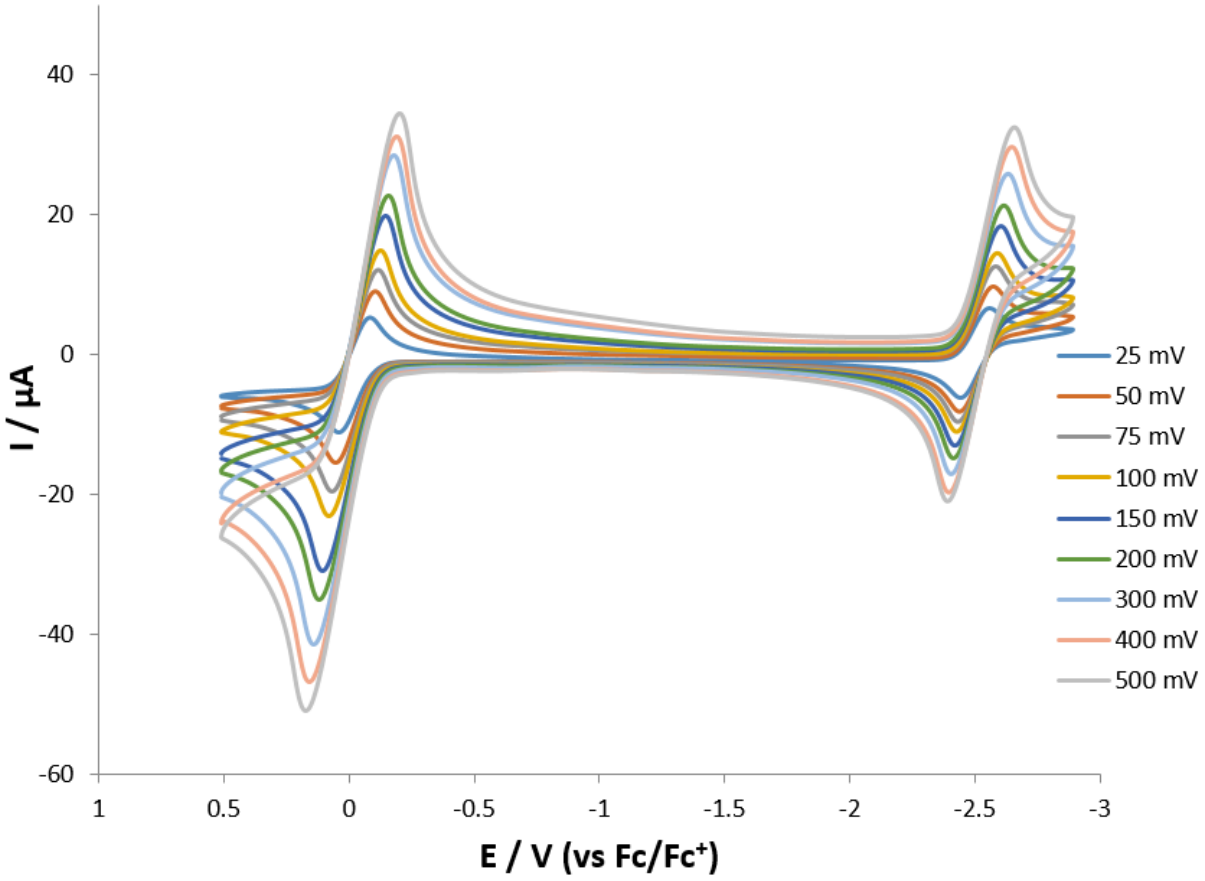

Table S10. Electrochemical data for **9** in DME (vs. $[Cp_2Fe]^{0/+}$).

Feature 1	**Scan rate, V/s**	**$E_{p,c}$, V**	**$E_{p,a}$, V**	**ΔE_p, V**	**$i_{p,c}/i_{p,a}$**
	0.025	-2.537	-2.421	0.116	1.02
	0.050	-2.551	-2.416	0.135	1.05
	0.075	-2.561	-2.41	0.151	1.07
	0.100	-2.568	-2.405	0.163	1.08
	0.150	-2.582	-2.398	0.184	1.08
	0.200	-2.594	-2.392	0.202	1.08
	0.300	-2.611	-2.383	0.228	1.09
	0.400	-2.626	-2.374	0.252	1.10
	0.500	-2.636	-2.369	0.267	1.10

Figure S30. Room temperature cyclic voltammogram of **10** in DME (vs internally referenced Cp_2Fe/Cp_2Fe^+ at $E_{1/2}$=0 V). (0.1M $[NBu_4][PF_6]$ as supporting electrolyte).

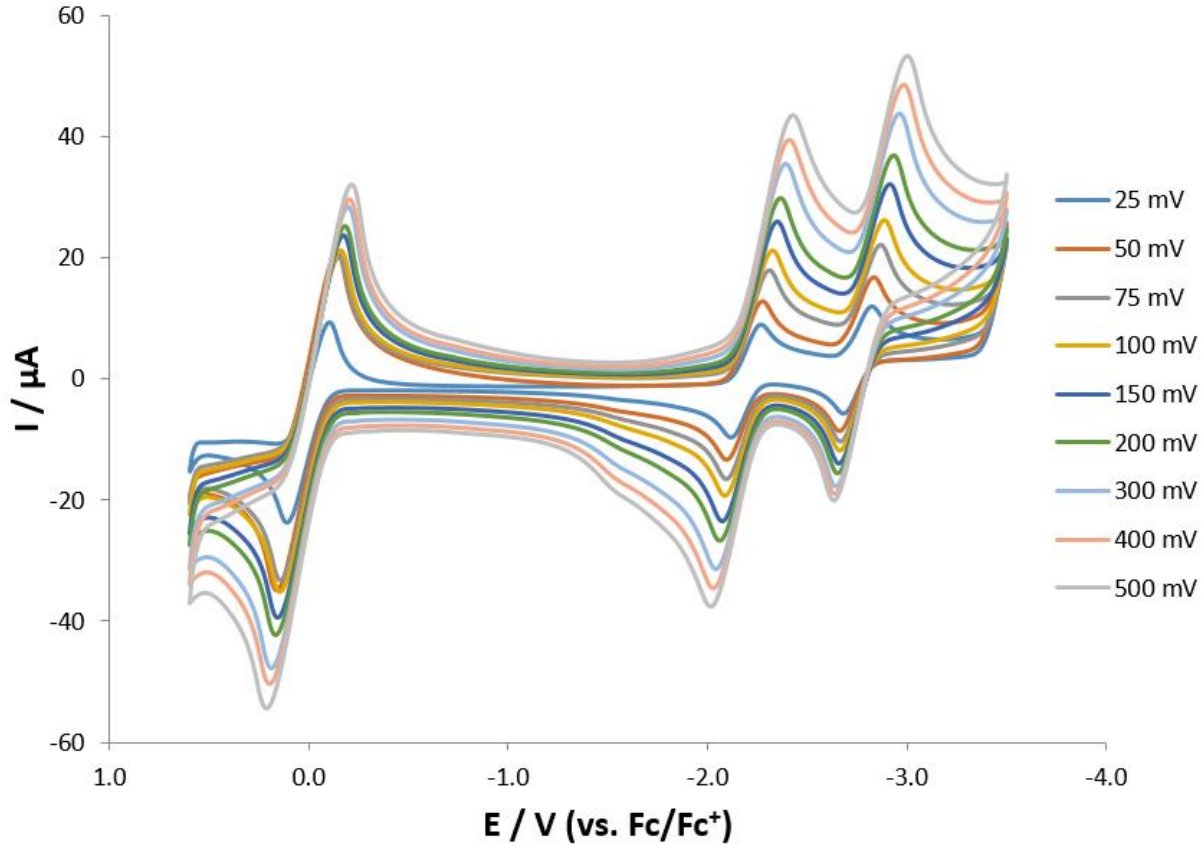

Table S11. Electrochemical data for **10** in DME (vs. $[Cp_2Fe]^{0/+}$).

Feature 1	**Scan rate, V/s**	**$E_{p,c}$, V**	**$E_{p,a}$, V**	**ΔE_p, V**	**$i_{p,c}/i_{p,a}$**
	0.025	-2.801	-2.657	0.144	1.03
	0.050	-2.838	-2.66	0.178	1.00
	0.075	-2.868	-2.666	0.202	0.97
	0.100	-2.886	-2.662	0.224	0.98
	0.150	-2.914	-2.658	0.256	0.99
	0.200	-2.933	-2.651	0.282	0.96
	0.300	-2.962	-2.642	0.32	0.94
	0.400	-2.982	-2.637	0.345	0.93
	0.500	-3.001	-2.632	0.369	0.92
Feature 2	**Scan rate, V/s**	**$E_{p,c}$, V**	**$E_{p,a}$, V**	**ΔE_p, V**	**$i_{p,c}/i_{p,a}$**
	0.025	-2.244	-2.094	0.15	1.10
	0.050	-2.275	-2.094	0.181	1.18
	0.075	-2.309	-2.093	0.216	1.14
	0.100	-2.325	-2.085	0.24	0.72
	0.150	-2.348	-2.072	0.276	1.02
	0.200	-2.365	-2.059	0.306	1.05
	0.300	-2.391	-2.04	0.351	1.05
	0.400	-2.409	-2.027	0.382	0.97
	0.500	-2.427	-2.014	0.413	0.94

Figure S31. Room temperature cyclic voltammogram of **11** in DME (vs internally referenced Cp_2Fe/Cp_2Fe^+ at $E_{1/2}$=0 V). (0.1M $[NBu_4][PF_6]$ as supporting electrolyte).

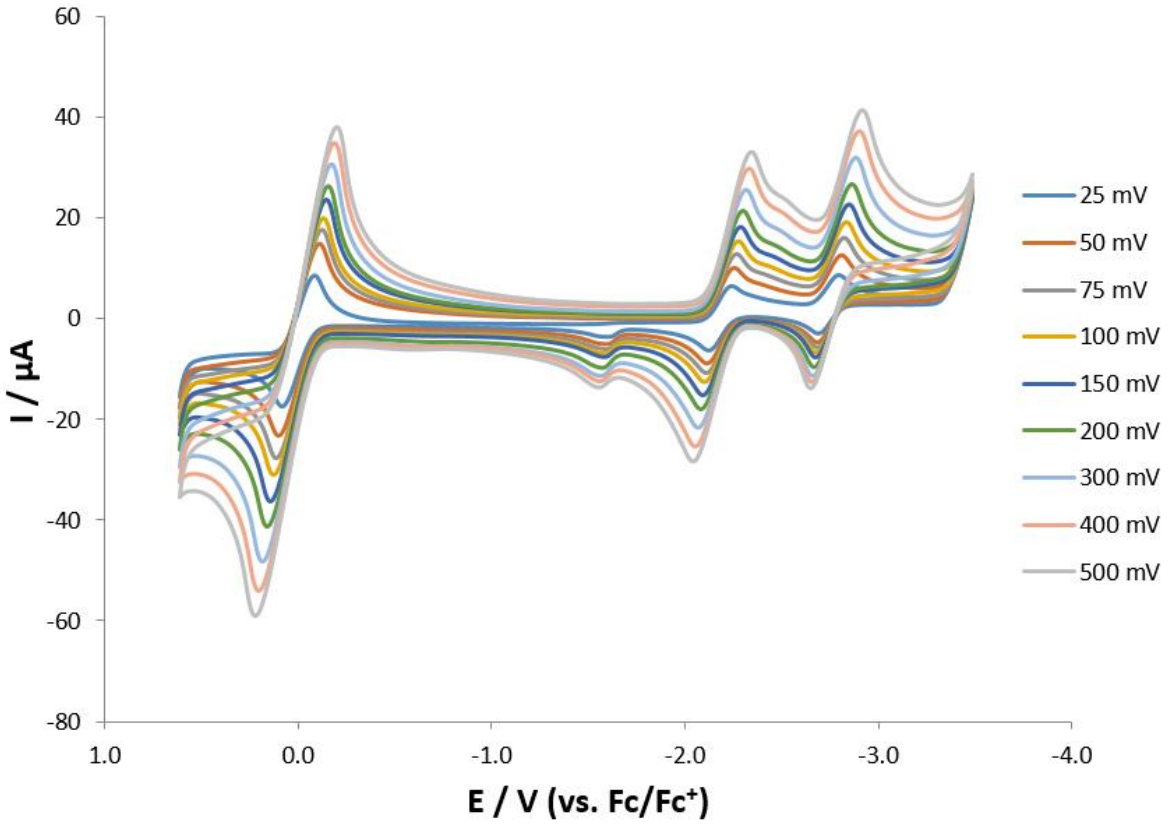

Table S12. Electrochemical data for **11** in DME (vs. $[Cp_2Fe]^{0/+}$).

Feature 1	**Scan rate, V/s**	**$E_{p,c}$, V**	**$E_{p,a}$, V**	**ΔE_p, V**	**$i_{p,c}/i_{p,a}$**
	0.025	-2.799	-2.693	0.106	1.04
	0.050	-2.813	-2.687	0.126	1.02
	0.075	-2.827	-2.687	0.140	1.07
	0.100	-2.838	-2.681	0.157	1.07
	0.150	-2.852	-2.678	0.174	1.06
	0.200	-2.867	-2.671	0.196	1.02
	0.300	-2.887	-2.663	0.224	1.02
	0.400	-2.906	-2.658	0.248	0.97
	0.500	-2.921	-2.653	0.268	0.96
Feature 2	**Scan rate, V/s**	**$E_{p,c}$, V**	**$E_{p,a}$, V**	**ΔE_p, V**	**$i_{p,c}/i_{p,a}$**
	0.025	-2.245	-2.126	0.119	1.06
	0.050	-2.258	-2.117	0.141	1.14
	0.075	-2.270	-2.113	0.157	1.16
	0.100	-2.280	-2.104	0.176	1.13
	0.150	-2.291	-2.095	0.196	1.05
	0.200	-2.303	-2.085	0.218	1.17
	0.300	-2.319	-2.071	0.248	1.14
	0.400	-2.334	-2.056	0.278	1.09
	0.500	-2.347	-2.045	0.302	1.07

Figure S32. Room temperature cyclic voltammogram of **12** in DME (vs internally referenced Cp_2Fe/Cp_2Fe^+ at $E_{1/2}$=0 V). (0.1M $[NBu_4][PF_6]$ as supporting electrolyte).

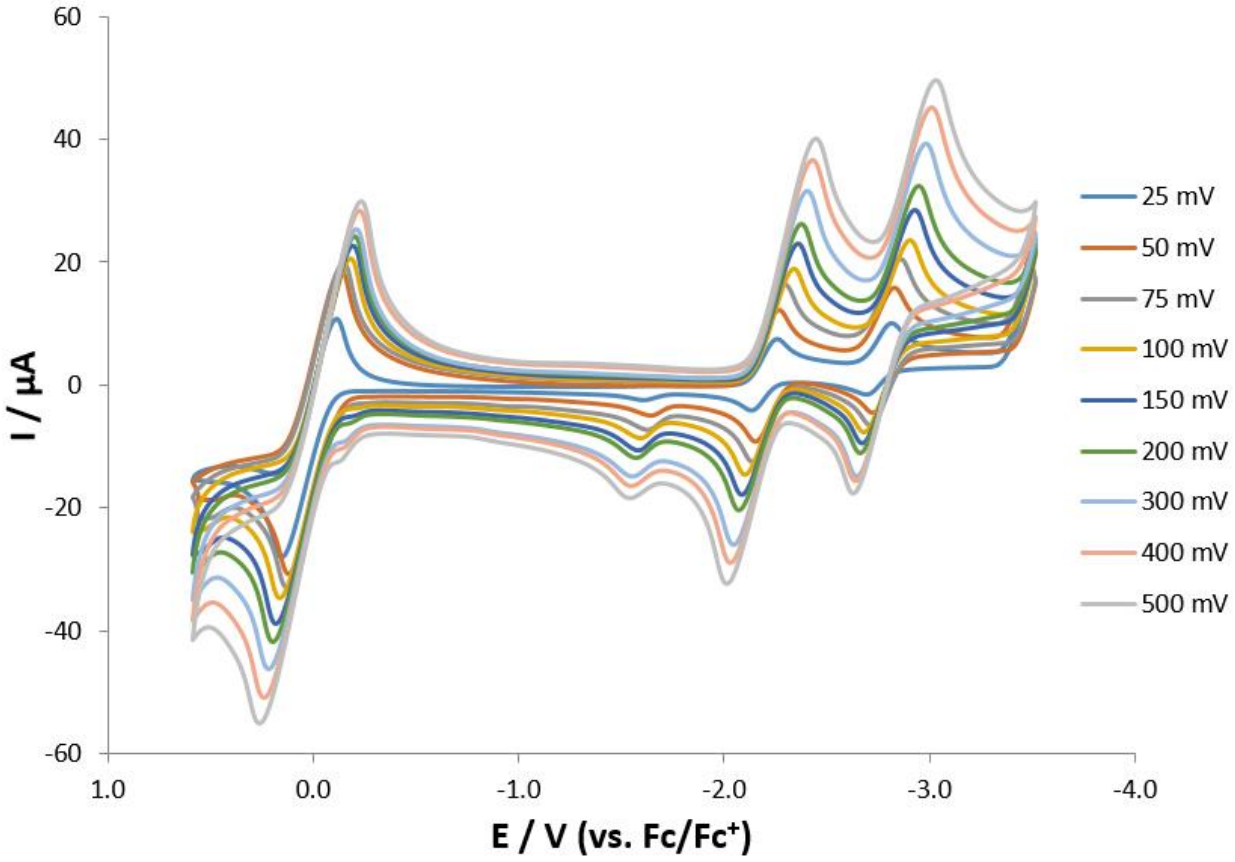

Table S13 Electrochemical data for **12** in DME (vs. $[Cp_2Fe]^{0/+}$).

Feature 1	**Scan rate, V/s**	**$E_{p,c}$, V**	**$E_{p,a}$, V**	**ΔE_p, V**	**$i_{p,c}/i_{p,a}$**
	0.025	-2.82	-2.697	0.123	1.79
	0.050	-2.864	-2.696	0.168	1.20
	0.075	-2.891	-2.688	0.203	1.10
	0.100	-2.909	-2.684	0.225	1.08
	0.150	-2.933	-2.676	0.257	1.06
	0.200	-2.952	-2.666	0.286	1.03
	0.300	-2.987	-2.649	0.338	1.01
	0.400	-3.015	-2.644	0.371	0.99
	0.500	-3.035	-2.633	0.402	0.97
Feature 2	**Scan rate, V/s**	**$E_{p,c}$, V**	**$E_{p,a}$, V**	**ΔE_p, V**	**$i_{p,c}/i_{p,a}$**
	0.025	-2.65	-2.137	0.513	1.62
	0.050	-3.06	-2.126	0.934	1.17
	0.075	-2.329	-2.113	0.216	1.29
	0.100	-2.344	-2.106	0.238	1.27
	0.150	-2.365	-2.091	0.274	1.21
	0.200	-2.381	-2.077	0.304	1.23
	0.300	-2.41	-2.05	0.36	1.19
	0.400	-2.435	-2.035	0.4	1.26
	0.500	-2.451	-2.018	0.433	1.24

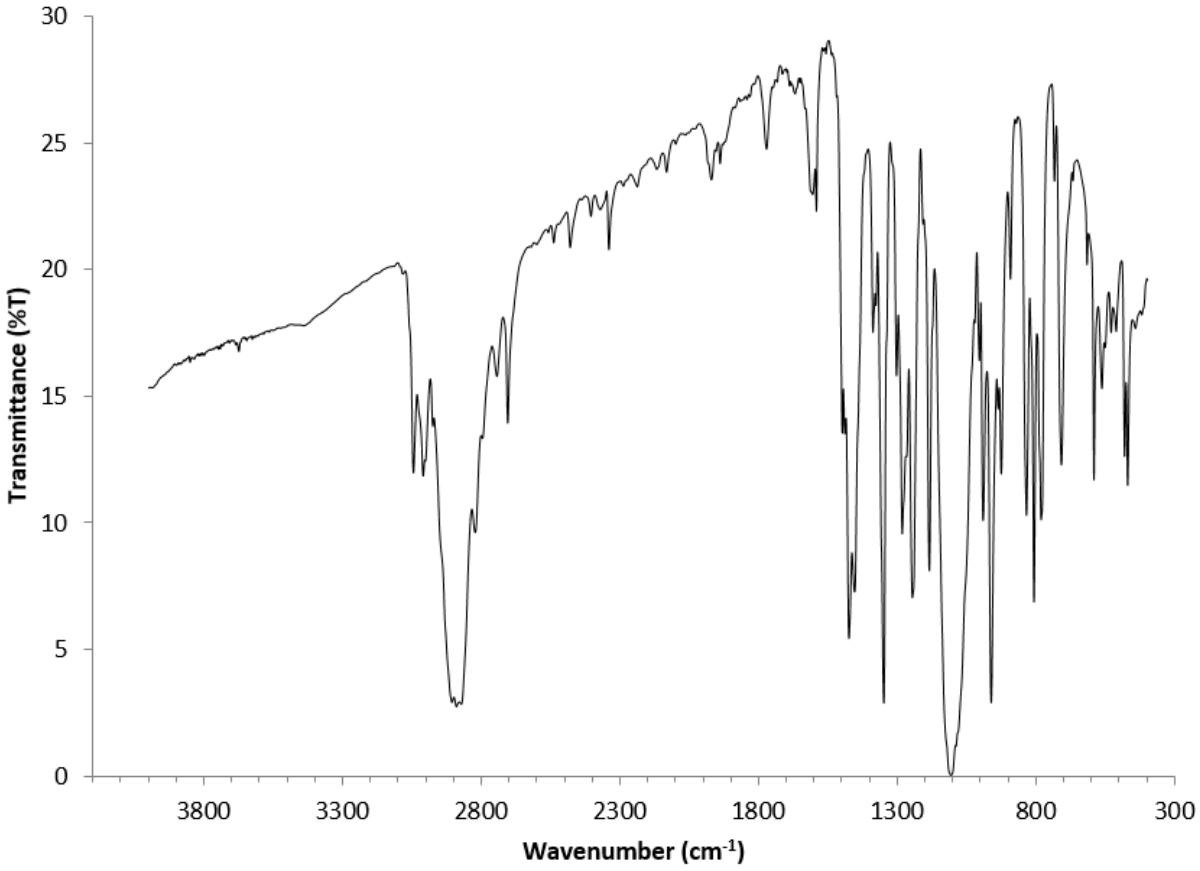

Figure S33. IR spectrum (KBr pellet) of **1**.

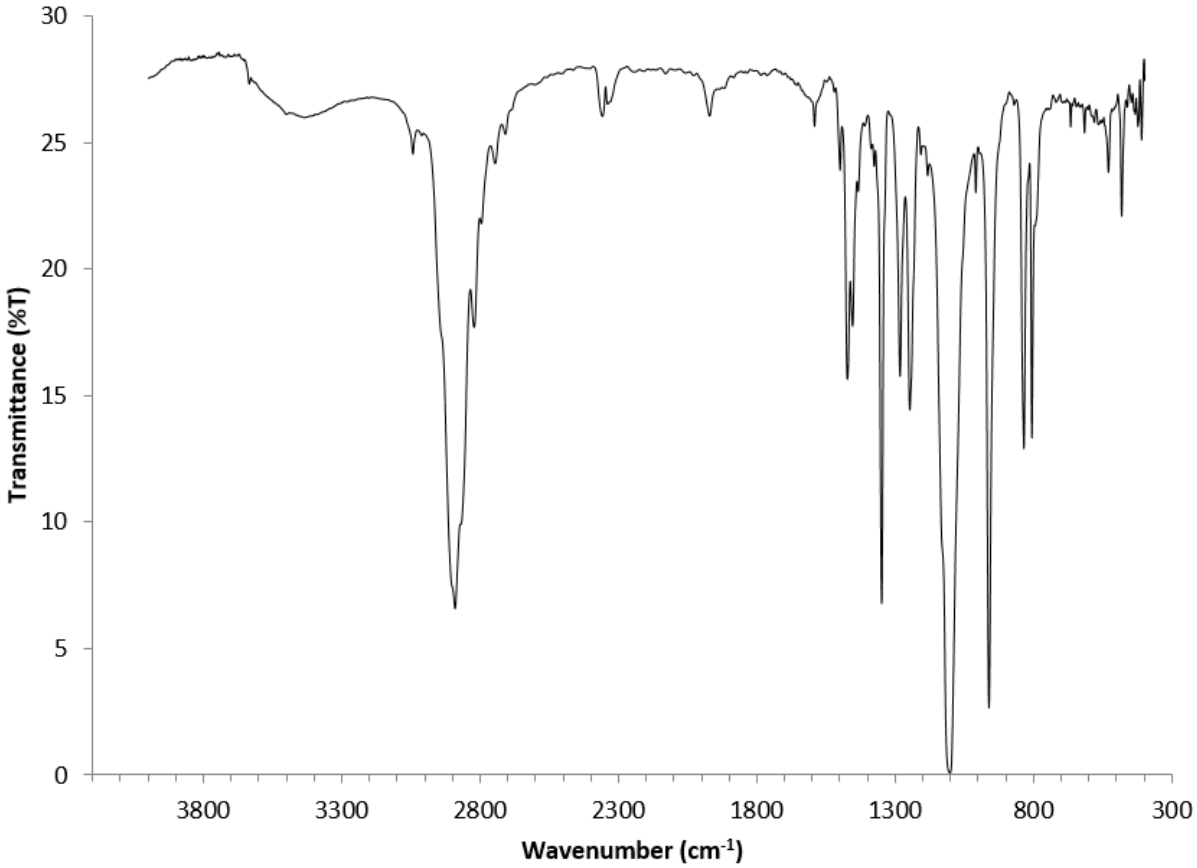

Figure S34. IR spectrum (KBr pellet) of **2**.

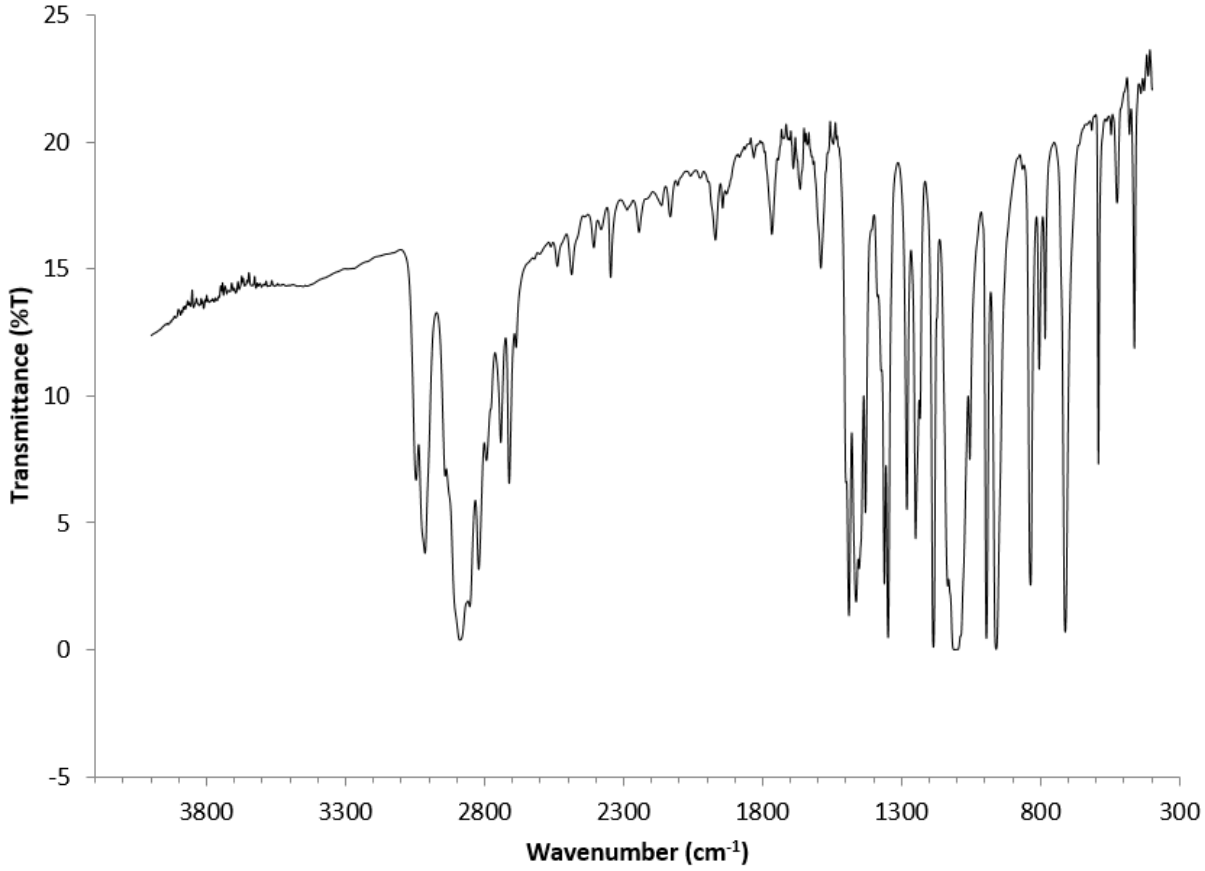

Figure S35. IR spectrum (KBr pellet) of **3**.

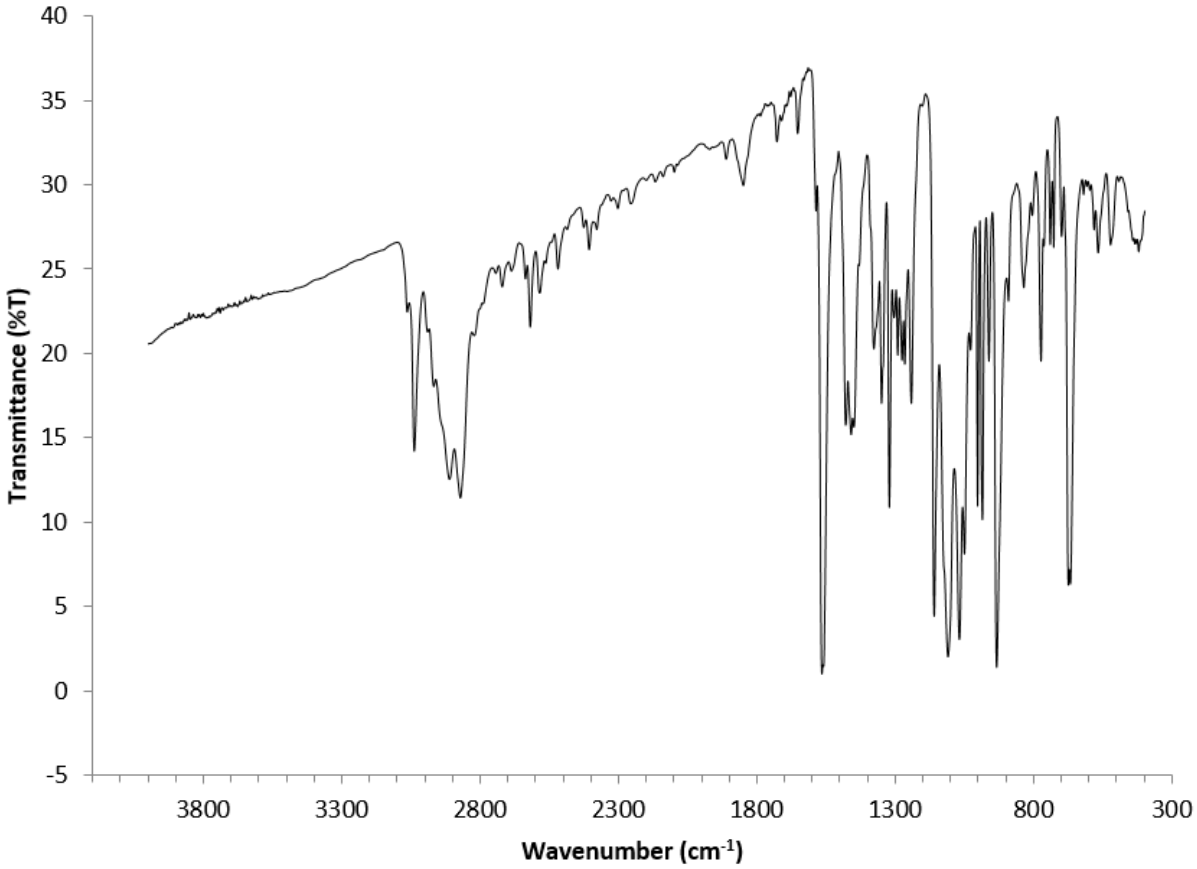

Figure S36. IR spectrum (KBr pellet) of **4**.

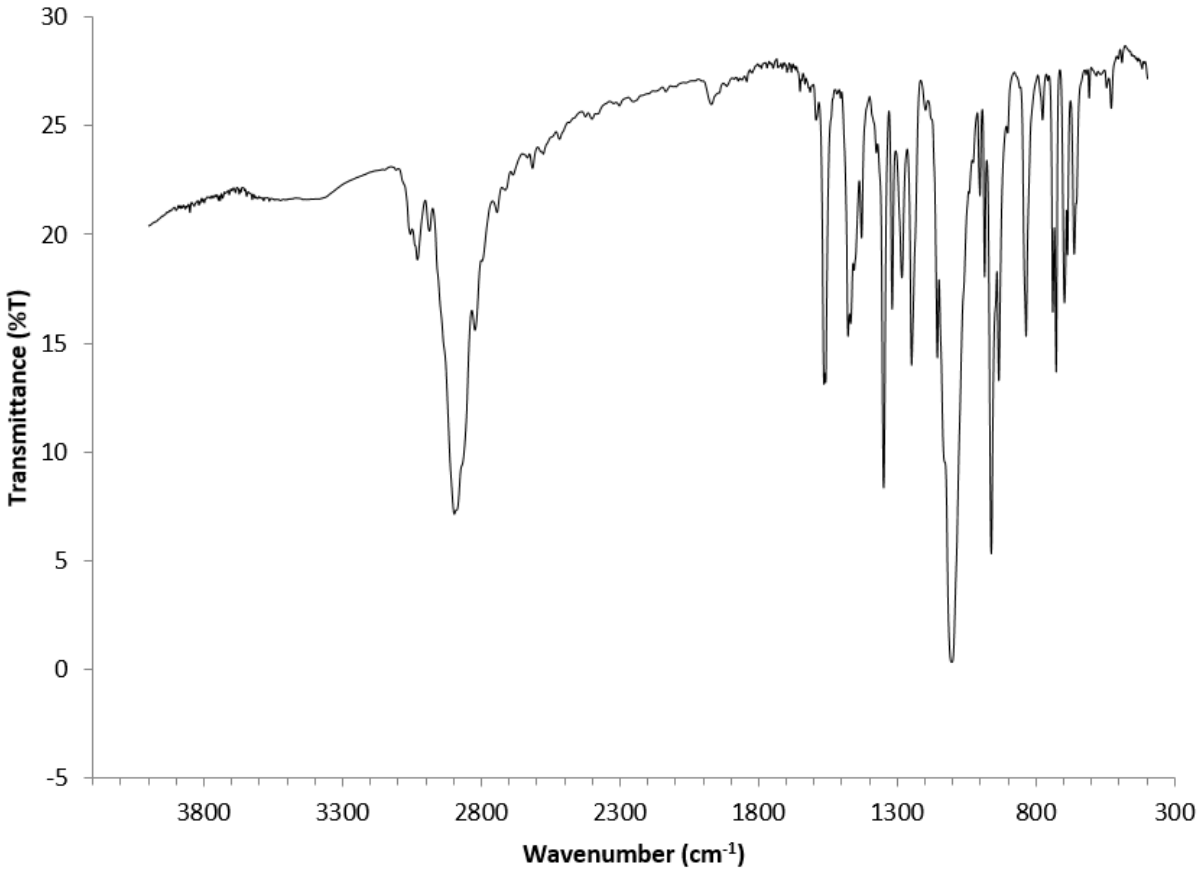

Figure S37. IR spectrum (KBr pellet) of **5.**

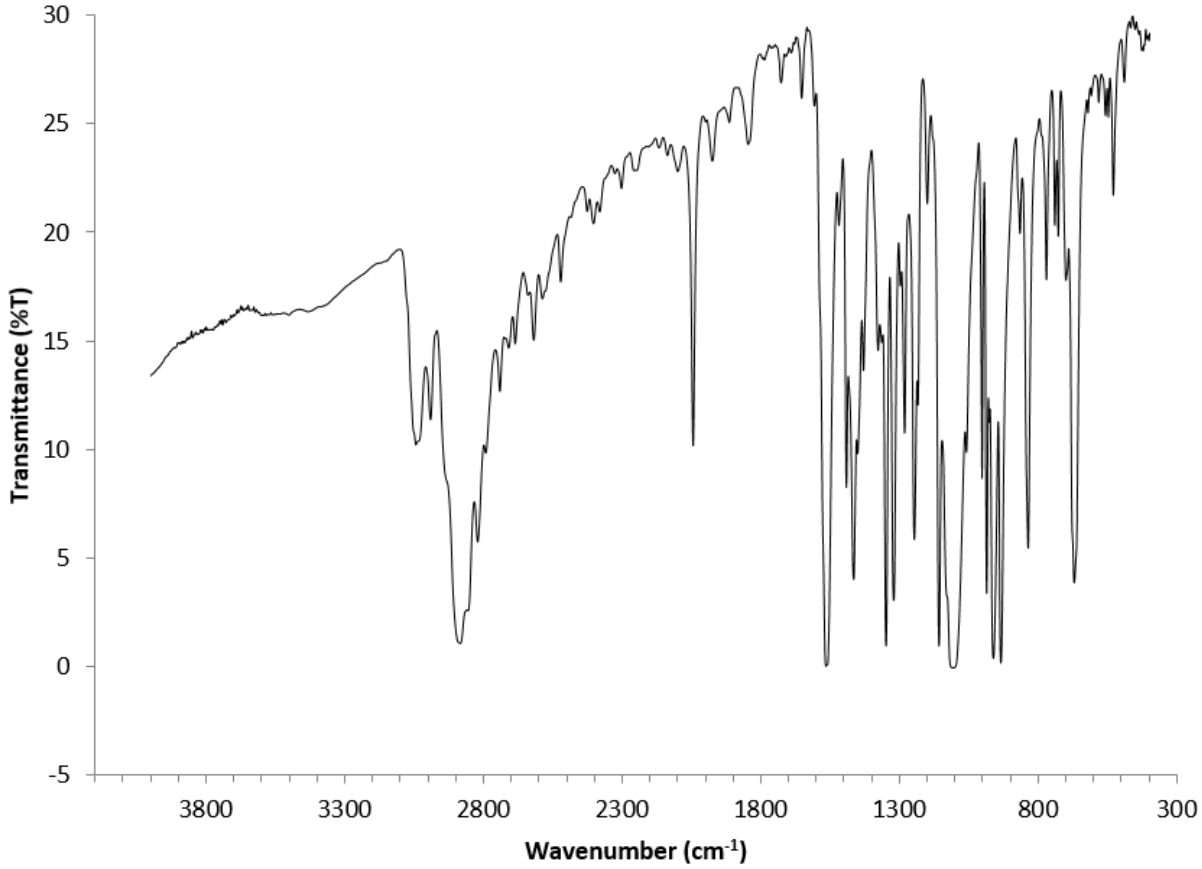

Figure S38. IR spectrum (KBr pellet) of **6.**

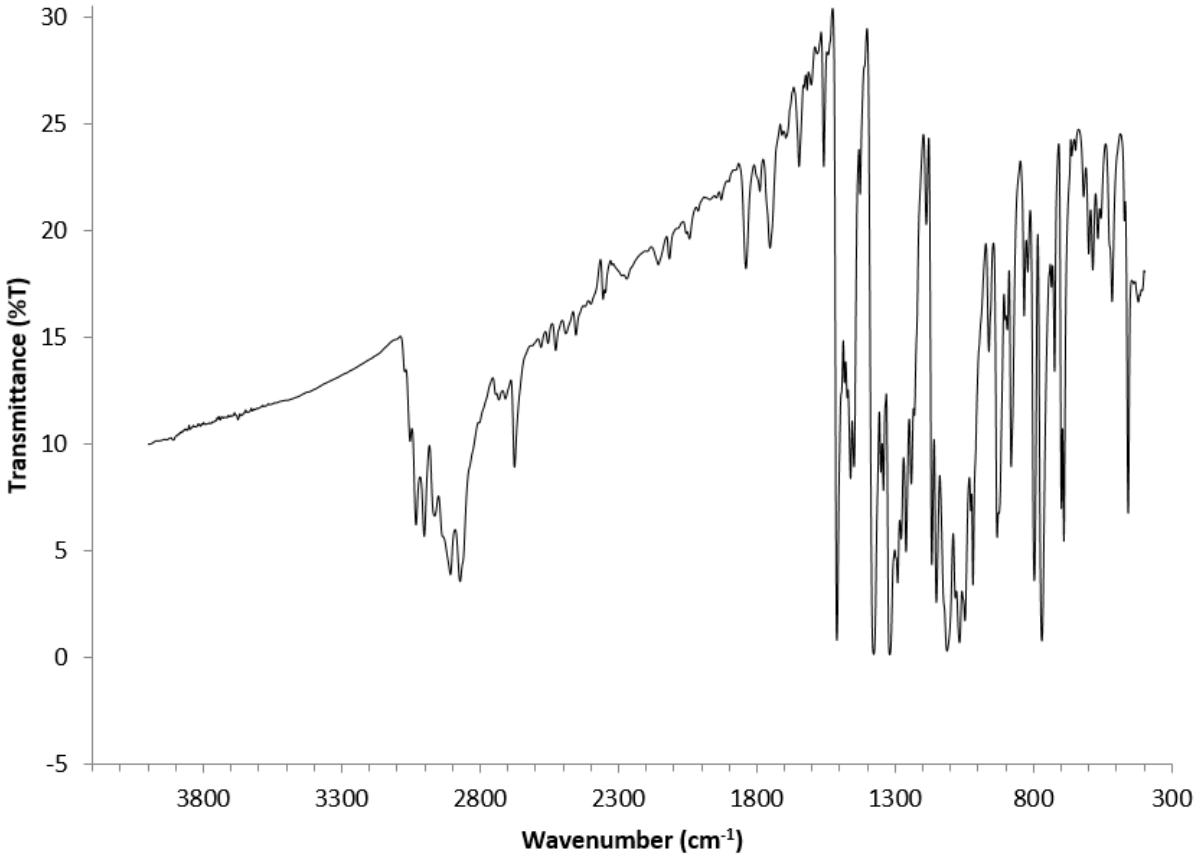

Figure S39. IR spectrum (KBr pellet) of **7.**

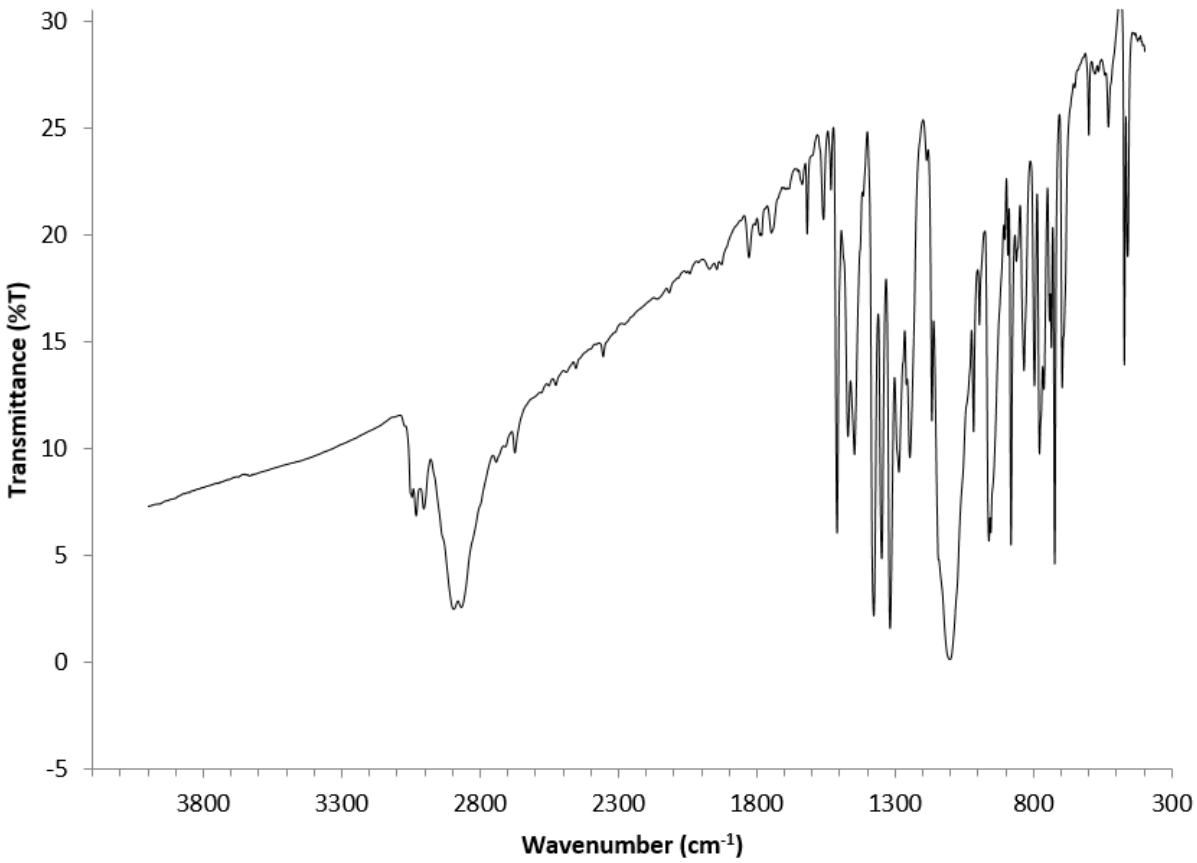

Figure S40. IR spectrum (KBr pellet) of **8.**

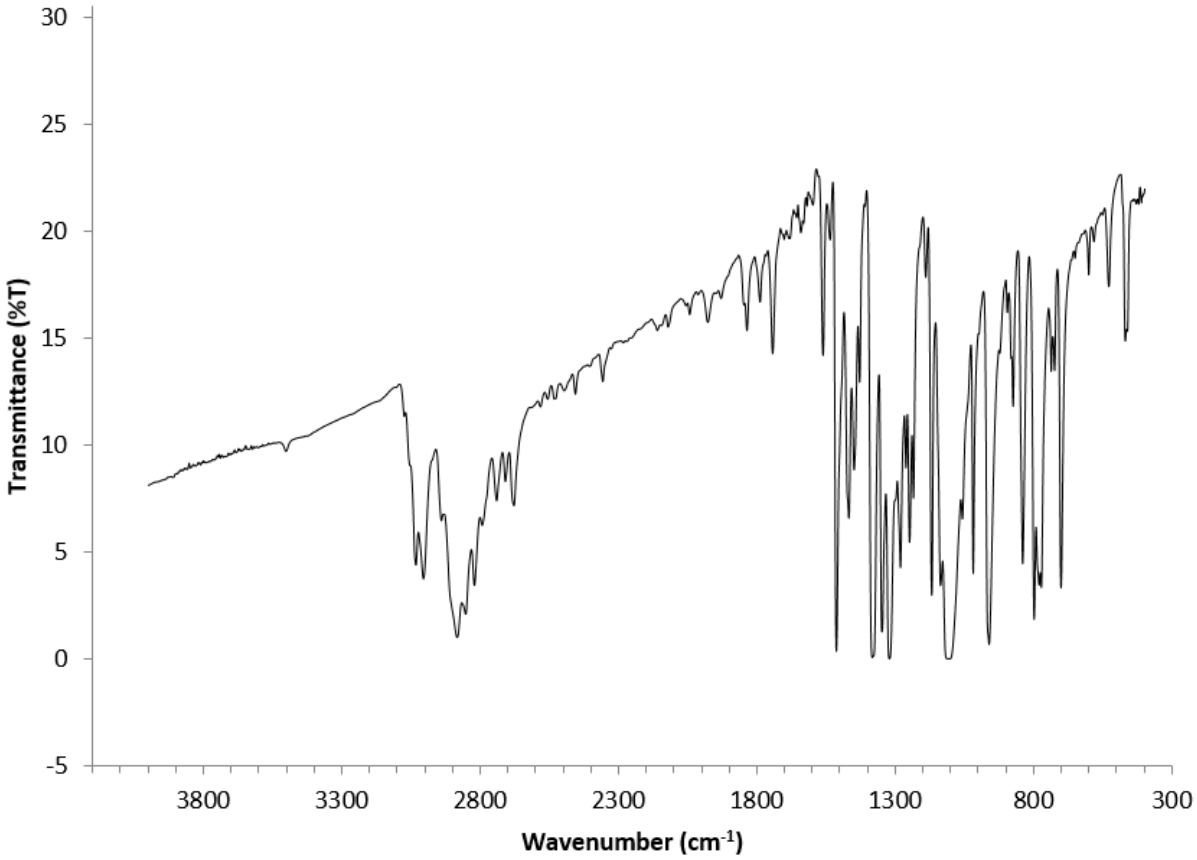

Figure S41. IR spectrum (KBr pellet) of **9.**

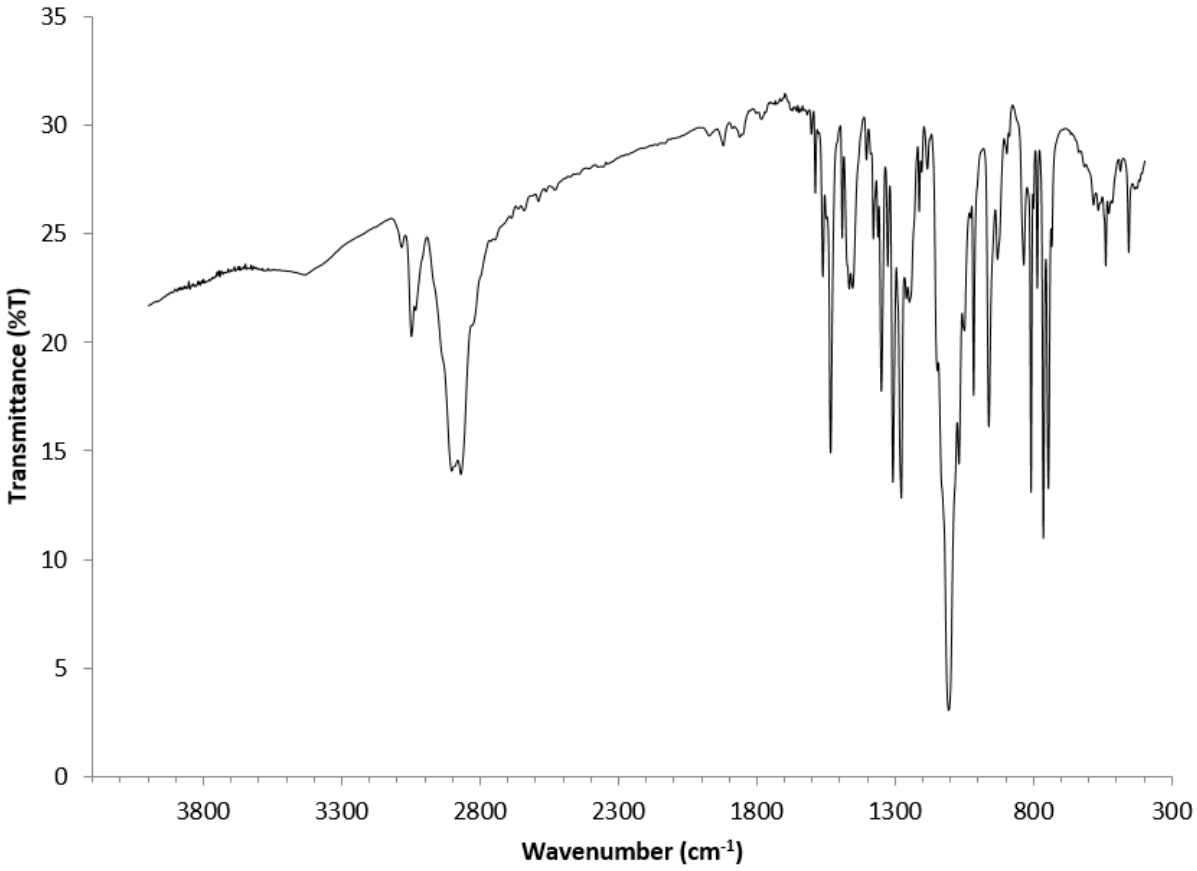

Figure S42. IR spectrum (KBr pellet) of **10.**

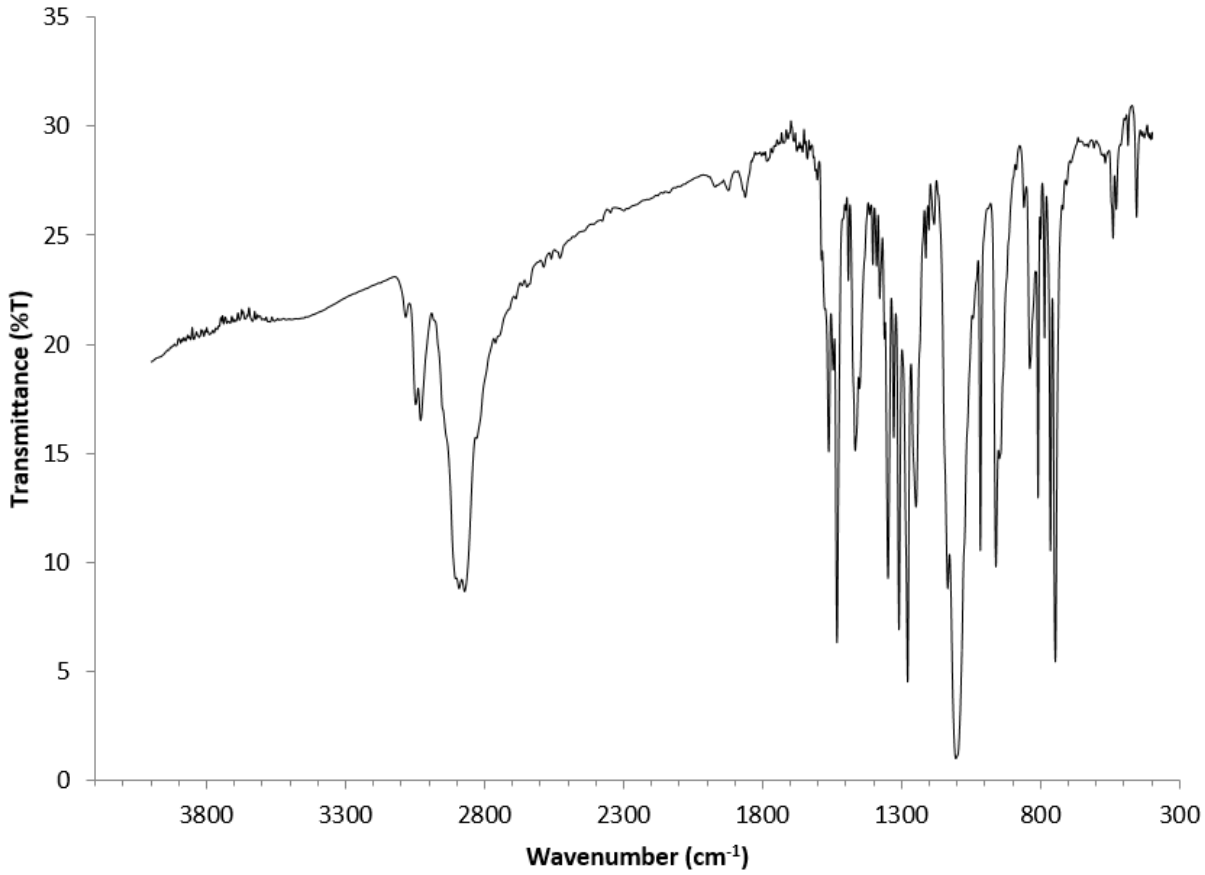

Figure S43. IR spectrum (KBr pellet) of **11.**

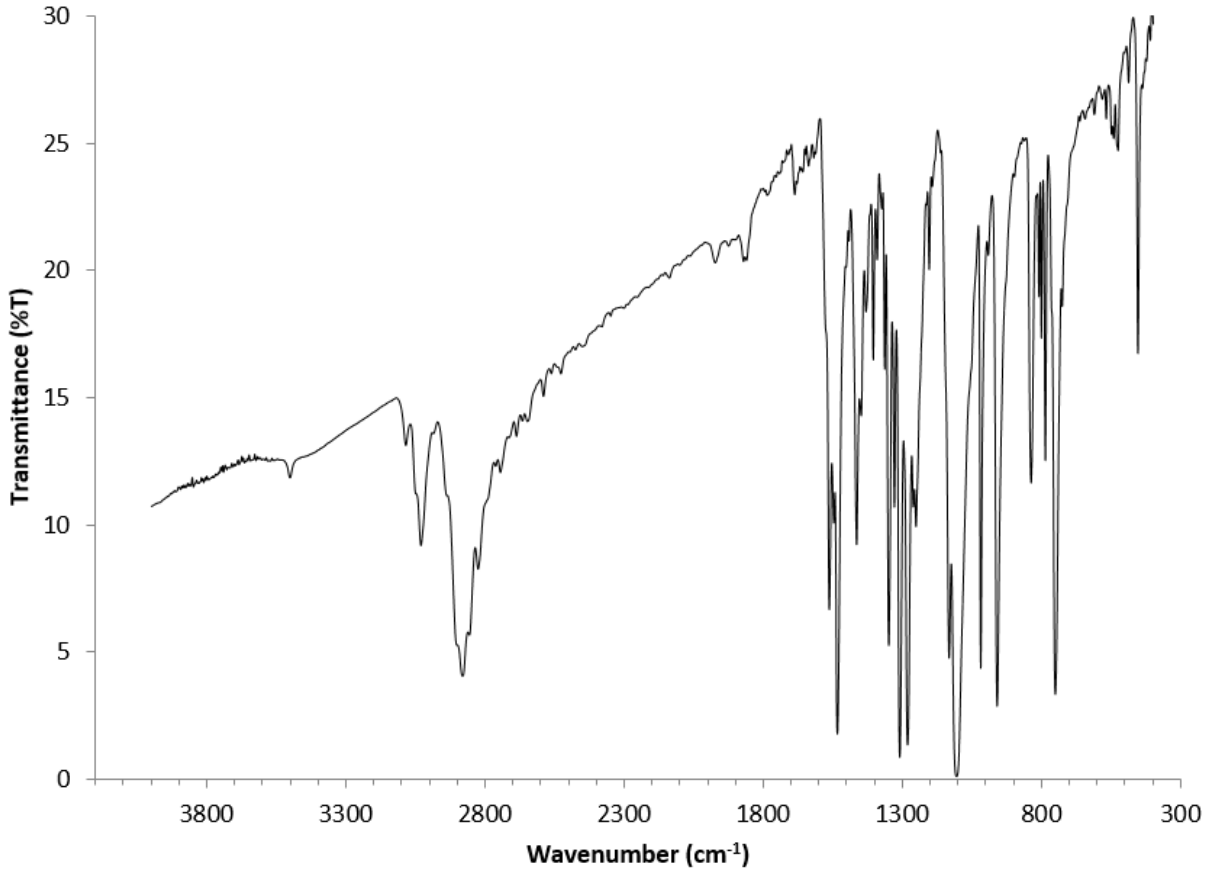

Figure S44. IR spectrum (KBr pellet) of **12.**

References

1. Gokel, G. W.; Cram, D. J.; Liotta, C. L.; Harris, H. P.; Cook, F. L. *J. Org.Chem.* 1974, *39*, 2445.
2. *SMART Apex II*, Version 2.1; Bruker AXS Inc.: Madison, WI
3. *SAINT Software User's Guide*, Version 7.34a; Bruker AXS Inc.: Madison, WI
4. Blessing, R. *Acta Crystallogr. A* 1995, *A51*.
5. Sheldrick, G. M. *SHELXTL*, 6.12; Bruker Analytical X-Ray Systems, Inc.: Madison, WI
6. Dolomanov, O. V.; Bourhis, L. J.; Gildea, R. J.; Howard, J. A. K.; Puschmann, H. *J. Appl. Cryst.* 2009, *42*, 339.